

UV LASER-INDUCED DNA PHOTOCHEMISTRY

1991

MASNYK



UNIFORMED SERVICES UNIVERSITY OF THE HEALTH SCIENCES

F. EDWARD HÉBERT SCHOOL OF MEDICINE

4301 JONES BRIDGE ROAD

BETHESDA, MARYLAND 20814-4799



APPROVAL SHEET

GRADUATE EDUCATION

TEACHING HOSPITALS

WALTER REED ARMY MEDICAL CENTER
NAVAL HOSPITAL, BETHESDA
MALCOLM GROW AIR FORCE MEDICAL CENTER
WILFORD HALL AIR FORCE MEDICAL CENTER

Title of Dissertation: "UV Laser-Induced DNA Photochemistry"

Name of Candidate: Taras Masnyk
Doctor of Philosophy Degree
May 13, 1991

Dissertation and Abstract Approved:

Kathleen V Holmes
Committee Chairperson

5/13/91

Date

Robert M. Freedman
Committee Member

5/13/91

Date

John P. Price
Committee Member

5/13/91

Date

William J. De Mene
Committee Member

5/13/91

Date

D. Samad
Committee Member

5/13/91

Date

Kenneth W. Miller
Committee Member

5/13/91

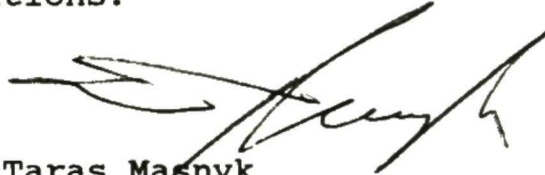
Date



The author hereby certifies that the use of any copyrighted material in the thesis manuscript entitled:

"UV Laser-Induced DNA Photochemistry"

beyond brief excerpts is with the permission of the copyright owner, and will save and hold harmless the Uniformed Services University of the Health Sciences from any damage which may arise from such copyright violations.



Taras Masnyk
Department of Pathology
Uniformed Services University
of the Health Sciences

ABSTRACT

Title of Dissertation: UV Laser-Induced DNA Photochemistry

Taras Masnyk, Doctor of Philosophy, 1991

Dissertation directed by: Kenneth W. Minton, M.D.

Associate Professor

Department of Pathology

Previous studies examining the effects of UV laser irradiation of nucleosides and nucleotides have determined that qualitative and quantitative differences exist between irradiation at low and high intensities. Multi-photon events involving the singlet and triplet excited states of DNA bases occur following irradiation at high intensity, leading to degradation of bases due to intra-molecular bond cleavage; such events are not seen following irradiation at low intensity. My aim in this work was to extend these studies to conditions of interest to biologists. I irradiated salmon sperm and plasmid DNA in aqueous solution at low (3.15×10^7 W/m²), intermediate (2.5×10^9 and 1.16×10^{10} W/m²), and high (1.25×10^{11} W/m²) intensities, using a KrF excimer laser emitting at 248 nm.

Following irradiation, DNA damage was assayed, with the following findings: 1) pyrimidine cyclobutane dimer and bipyrimidine T(6-4)C photoadduct formation was reduced following irradiation at high intensity relative to low

intensity; 2) free thymine and thymine fragments were released from DNA following irradiation at high intensity, but not at low intensity; 3) DNA strand break formation increased with increasing intensity; 4) double-stranded breaks occurred in DNA following irradiation at high intensity. A mathematical model describing the effect of high intensity UV radiation on plasmid DNA conformation was developed and fit to experimental data on strand breaks. Using the model, dose constants for single- and double-stranded breaks were determined and found to increase with intensity.

These results are consistent with the absorption of a second photon by long-lived triplet excited states of DNA following irradiation at high intensity, but not low intensity. Absorption of two photons leads to the depopulation of triplet excited states in DNA through ionization and fragmentation of bases, causing decreased levels of pyrimidine dimer formation and increased amounts of strand breakage in DNA. These results generally agree with earlier experiments using DNA components, and help extend our understanding of DNA-UV light interactions.

UV Laser-Induced DNA Photochemistry

by

Taras Masnyk

Dissertation submitted to the Faculty of the Department of Pathology in the Molecular Pathobiology Graduate Program of the Uniformed Services University of the Health Sciences in partial fulfillment of the requirements for the degree of Doctor of Philosophy, 1991

This work is dedicated to my father. When I was a young boy and kept asking "Why?", he did not start answering "Because", but instead gave me an encyclopedia. Thus he started me on a journey of discovery that continues today.

D'iakuju, tatu!

Acknowledgments

I would like to thank the members of the Laser Biophysics Department at USUHS. They provided material support for my project, and helped keep an often recalcitrant laser operating properly.

I would also like to thank the members of my family- my parents, my sister, my aunts and uncles. They provided support and encouragement, especially during difficult periods over the last several years, and helped me see this project to its completion.

Special thanks to my advisor, Dr. Kenneth Minton. To him I owe a great debt. Without his support, encouragement, discussion, understanding, and occasional threats, this work would not have been possible. Thank you, Ken, for your tutelage and patience.

Final thanks to my wife. She stood by me, and eased my journey through graduate school. Without her love, this work would not have been worth doing.

TABLE OF CONTENTS

I. Introduction.....	1
II. Excited States.....	16
III. DNA Photoproducts.....	30
IV. Material and Methods.....	36
V. Results.....	54
VI. Discussion.....	91
VII. Bibliography.....	121

FIGURES

Figure 1- Schematic Diagram of Atomic Excitation.....	19
Figure 2- The Singlet Excited State.....	22
Figure 3- The Triplet Excited State.....	24
Figure 4- Schematic of Relaxation Modes.....	26
Figure 5- The Major DNA Photoproducts.....	31
Figure 6- Laser Set-Up.....	39
Figure 7- Acid Hydrolysis of DNA.....	42
Figure 8- Formation of Thymine-thymine Cyclobutane Dimers (T<>T) in KrF Laser Irradiated DNA....	56
Figure 9- Formation of Thymine-cytosine Cyclobutane Dimers (T<>C) in KrF Laser Irradiated DNA....	57
Figure 10- Formation of T(6-4)C in Laser Irradiated DNA....	59
Figure 11- TLC Separation of Thymine and Thymine Decomposition Products Released from DNA Following Laser Irradiation.....	62
Figure 12- Gel Electrophoresis of Irradiated Samples.....	67
Figure 13- The Poisson Distribution.....	70
Figure 14- Gel Electrophoresis of DNase I Digests.....	74
Figure 15- Results of Curve Fitting.....	77
Figure 16- Gel Electrophoresis of Irradiated Samples.....	83
Figure 17- Effect on k_1 and k_2 of Varying Overlap Values...	86
Figure 18- Values for k_1 and k_2 at Various Intensities.....	88
Figure 19- Triplet Sensitization.....	104
Figure 20- Results of Curve Fitting to Independent Data....	111

ABBREVIATIONS

B- the overlap value, the minimum number of nucleotides separating two single stranded breaks on opposite strands without double stranded scission occurring

D- the total dose delivered to the sample

DSB('s)- double stranded break(s)

et- energy transfer

eV- electron volts

G₀- the ground state of an atom or molecule, equivalent to S₀

hv- a photon

ic- internal conversion

isc- intersystem crossing

J/m², Jm⁻²- joules per meter squared

k₁- the single stranded break constant (breaks/base/J/m²)

k₂- the double stranded break constant (breaks/base/J/m²)

M- the number of bases per DNA molecule

ms- millisecond (10⁻³s)

nm- nanometer (10⁻⁹m)

ns- nanosecond (10⁻⁹s)

pfu- plaque forming unit

ps- picosecond (10⁻¹²s)

RF- replicative form

S₀- the ground state of an atom or molecule, equivalent to G₀

S₁- the first singlet excited state

S_2 - the second and subsequent singlet excited states

SSB('s)- single stranded break(s)

T_1 - the first triplet excited state

T_2 - the second and subsequent triplet excited states

T^C , $T<>C$ - a thymine-cytosine cyclobutane dimer

T^T , $T<>T$ - a thymine-thymine cyclobutane dimer

$T(6-4)C$ - a 6-4'-[pyrimidine-2'-one]thymine photoadduct

UV- ultraviolet

W/m^2 , Wm^{-2} - watts per meter squared, $1 W/m^2 = 1 J/m^2/s$

INTRODUCTION

At conventional UV intensities, DNA photochemistry is one photon in nature; that is, a single photon absorbed by a DNA base produces an electronic excited state that decays by various pathways to the ground state (Häder and Tevini, 1987). In a fraction of instances, alterations in covalent bonds occur, yielding a number of well described photoproducts (Wang, 1976b). Recently, halogen-noble gas excimer lasers and powerful Nd:YAG lasers that produce ultraviolet radiation have been developed (Brau, 1984; Pummer et al., 1984). Such lasers can deliver the same number of photons (the same dose) at a relatively low intensity over long time periods, or at high intensity over short time periods. Sufficiently high intensities provide a high statistical probability that during the excited state lifetime, a second photon will be encountered by an excited DNA base, or by nearby bases, thereby promoting that base to an even more energetic excited state (Letokhov, 1983). These more energetic excited states have different decay pathways and result in different forms of DNA damage than are usually encountered (Nikogosyan, 1990). For a given number of photons (an equivalent dose), there are quantitative and qualitative differences in DNA damage,

depending on whether they are delivered over a short time period (at high intensity) or a long time period (at low intensity).

The formation of photoproducts from thymine and other nucleic acids components has been relatively well characterized with regard to the contribution of singlet and triplet excited states (Wang, 1976b). In contrast, the excited state precursors of photoproducts under conditions of interest to biologists (DNA in aqueous solution or in cells) remain unresolved due to inherent technical difficulties (Wang, 1976a). Unlike studies on free bases or nucleotides, in DNA the substrate is not homogeneous; studies using diffusion and varying concentrations of DNA bases are precluded since bases are fixed with respect to each other through covalent linkages; the efficacy of triplet state quenchers such as Mn^{++} , useful in studies on free bases and nucleotides, is reduced, probably due to steric hinderance (Fisher and Johns, 1970). The introduction of excimer and powerful Nd:YAG lasers that emit UV light and their use in the study of DNA photochemistry has helped circumvent these difficulties, and led to an increased understanding UV-DNA interactions (see Nikogosyan, 1990, for review). Depending on their design, such lasers are capable of achieving intensities from 10^{11} W/m^2 to 10^{14} W/m^2 , much higher than the

intensities achievable with conventional UV light sources (low pressure mercury vapor lamp, maximum intensity on the order of 10 W/m^2).

Several investigators have examined the effect of UV laser irradiation on nucleic acids components. Menshonkova et al. (1980) used the fourth harmonic of a Nd:YAG laser, in a 10 ns pulse, to irradiate thymidine, adenosine, and 2'-deoxy-adenosine at 266 nm, achieving intensities of up to $1.24 \times 10^{11} \text{ W/m}^2$. Following irradiation, they analyzed the resultant photoproducts by thin layer chromatography, and found that irradiation at high intensity led to cleavage of the N-glycosidic bond, and to the degradation of the thymine and adenine bases. Budovskii et al. (1981) performed similar experiments, irradiating thymine and adenine, as well as their nucleoside analogues, using the same laser set-up and intensity noted above. They too found degradation of the bases and cleavage of the N-glycosylic bond. Budovskii and coworkers also performed two-dimensional thin layer chromatography, comparing the results of high intensity UV irradiation with gamma-ray irradiation of thymine and adenine. They found that irradiation with high intensity UV light produced results similar to gamma-ray irradiation, suggesting that similar mechanisms of action were involved. Finally, they determined the intensity dependence of nucleic acids base

damage by following the optical density of the bases (A_{260}), and found a quadratic relationship, at intensities up to 10^{11} W/m². Both groups (Menshonkova et al., 1980; Budovskii et al., 1981) suggest that their results are best explained by the ionization of the irradiated base, following the absorption of a second photon by triplet excited state bases. Mathematical treatment of these and similar experiments by Rubin et al. (1981) demonstrated that such multi-photon events were indeed occurring via the triplet state under the conditions employed (irradiation at 266 nm, at 10^{10} - 10^{11} W/m² range, with a 10 ns pulse).

Harrison (1984) used a KrF excimer laser to irradiate uridylyl(3'-5')uridine (UpU) with nanosecond pulses at 248 nm, at intensities of 1.9×10^9 W/m² (low intensity) and 2.5×10^{11} W/m² (high intensity). Following irradiation, analysis by high pressure liquid chromatography and thin layer chromatography showed that irradiation at high intensity resulted in the cleavage of the N-glycosylic bond, and in occasional breakage of phosphodiester bonds. Irradiation at low intensity gave results similar to those seen following irradiation with conventional UV sources (low pressure mercury vapor lamp).

Nikogosyan et al. (1982) irradiated cytosine, thymine, adenine, guanine and uracil in aqueous solution, using the

fourth harmonic of a YAG laser to achieve picosecond pulses and intensities of up to 10^{14} W/m², or a KrF excimer laser to achieve nanosecond pulses and intensities of up to about 10^{11} W/m². By following changes in optical density of the bases after irradiation with either the picosecond or nanosecond laser, Nikogosyan and coworkers (1982) were able to determine the effect of these lasers on the five nucleic acid bases. They showed that the nucleic acid base degradation that occurs following irradiation with a laser emitting picosecond pulses (at intensities of up to 10^{14} W/m²) was due to the absorption of a second photon by bases that were in the singlet excited state, and involved photoionization of the base, with a minor contribution from the photoionization of water. On the other hand, irradiation with nanosecond pulses led to multi-photon events of bases in the triplet excited state, and occurred entirely through the photoionization of the base; there was no contribution from the photodissociation of water under those conditions.

In addition to the above studies on nucleic acid bases, nucleosides, and dinucleotides, other investigators have examined the effect of UV excimer laser irradiation on polynucleotides. Gurzadyan et al. (1981) used the fourth harmonic of a picosecond Nd:YAG laser (30 ps pulse at 266 nm) to irradiate λ and ϕ X174 bacteriophages and pBR322 plasmid DNA

at intensities of 10^{11} to 10^{13} W/m². They determined the mechanism of viral inactivation by growing the irradiated virus on bacterial hosts that were either capable or incapable of repairing pyrimidine dimers (the major form of lethal damage following irradiation under conventional conditions at low intensity). Their results showed that viral inactivation following irradiation at high intensity (10^{11} to 10^{13} W/m²) was due to the induction of single stranded breaks, and not due to the formation of pyrimidine dimers. In further support of this conclusion, gel electrophoresis of irradiated pBR322 plasmid DNA showed that the degree of strand breakage paralleled increasing viral inactivation following irradiation at increasing doses.

Nikogosyan and Gurzadyan (1984) used a picosecond laser emitting at 266 nm (the fourth harmonic of a Nd:YAG laser) to study the quantum yields of strand breaks in pBR322 plasmid DNA and in tobacco mosaic virus RNA, as well as the formation of intra-molecular crosslinks in C_D phage DNA. They also studied the quantum yield of thymine degradation following picosecond laser irradiation. The intensities achieved in their studies varied from 10^{10} to 10^{14} W/m². They found that the quantum yields of strand-breaks and crosslinks increased with increasing intensity, up to about 10^{12} W/m², at which point a plateau level was reached. They attributed the

plateau in quantum yields to the saturation of one of the steps in the excitations they were investigating. They also found the quantum yield for dimer formation in poly-dT began to decrease at a certain intensity (about 10^{12} W/m²), which was lower than a similar decrease seen in irradiated monomeric thymine (at 5×10^{13} W/m²). This was attributed to the migration of electronic excitation along the poly-dT polymer.

Similar experiments were performed by Zavilgelsky et al. (1984). They used picosecond and nanosecond lasers and low pressure mercury vapor lamps to irradiate poly-dT, C_b bacteriophage, λ bacteriophage, and pBR322 plasmid at intensities ranging from 10^1 to 10^{14} W/m². They found that the quantum yields for intra-molecular crosslink and single-strand break formation increased as intensity increased, once a threshold intensity of approximately 10^{11} W/m² was surpassed. On the other hand, the yield of pyrimidine dimers was unaffected by intensity, until a higher threshold intensity of 10^{12} W/m² was reached; at that point, the quantum yield for dimer formation began to decrease. Zavilgelsky and coworkers (1984) reasoned that the formation of cross-links and strand breaks was a multi-photonic process. These forms of damage occurred following the photoionization of a DNA base after it had absorbed the energy of two photons. The increase in quantum yields seen after irradiation by intensities above 10^{11}

W/m^2 reflected the transition from single- to multi-photon UV-DNA interactions. Pyrimidine dimers, on the other hand, are formed by single-photon excitation of DNA bases, as pyrimidine dimers are a common form of damage following irradiation at low intensity (10 W/m^2) (Fisher and Johns, 1976). Under the conditions Zavigelsky and coworkers (1984) used, the picosecond laser would induce multi-photon events involving the singlet excited state, while the nanosecond laser would induce multi-photon events involving triplet excited states. They reasoned that the high threshold (10^{12} W/m^2) required to achieve decreased quantum yields for dimer formation indicated that all low singlet excited states had to be depleted by promotion to higher singlet states to observe a significant drop in the formation of this single photon photoproduct. They proposed that this result demonstrated that all pyrimidine dimers are made exclusively through the singlet excited state.

Schulte-Frohlinde et al. (1985) studied the formation of strand breaks in poly-U following laser flash photolysis. A KrF laser was used to irradiate poly-U in aqueous solution at 248 nm in 20 ns pulses. Single-strand breaks were seen and their mechanism was investigated. Conductivity studies during irradiation demonstrated that the single-stranded breaks occurred as a result of the direct photoionization of uracil

residues, followed by the creation of reactive radical cations.

From the above discussion, it is clear that a number of different investigators used UV lasers to determine the effect of high intensity irradiation on DNA and DNA components. These studies have shed light on the nature of damage sustained by DNA and DNA components following irradiation at high intensity, and have shown that there are qualitative and quantitative differences between irradiation at high and low intensities. Also, these studies have provided some insights regarding the photochemical mechanisms of damage to nucleic acids and their constituent components, and the contributions of various excited states to the generation of UV photoproducts. However, the studies published by the time I started my work were limited. Most investigators examined the effect of high intensity irradiation on nucleic acid components- bases, nucleosides, nucleotides, oligonucleotides, or synthetic polynucleotides. Only a few studies were performed under conditions of interest to biologists- irradiation of DNA in aqueous solution (Gurzadyan et al., 1981; Nikogosyan and Gurzadyan, 1984; Zavilgelsky et al., 1984).

Gurzadyan et al. (1981) used gel electrophoresis to determine the extent of strand break formation in plasmid DNA

following high intensity UV irradiation. However, they did not quantitate the results of this electrophoresis; only showing photographs of their gels as support of their findings regarding the mechanism of bacteriophage inactivation following high intensity irradiation. Gurzadyan and coworkers (1981) also used nine different doses among three different intensities, such that results were not directly comparable, making it difficult to ascertain the relative contributions of dose and intensity to the DNA damage observed. Nikogosyan and Gurzadyan (1984) reported only the quantum yields for a number of different forms of DNA damage (intra-molecular cross-links, strand breaks, base degradation). They did not report any data on the actual amounts of damage sustained by their samples following irradiation, making it difficult to objectively evaluate their work. Zavilgelsky *et al.* (1984) did provide data regarding the level of damage induced in some of their experiments. However, their assays may have been less sensitive than other available methods of detecting damage to DNA and its components. For example, they measured the level of pyrimidine dimer formation by measuring the change in absorption of DNA following the reversion of dimers to monomers by low intensity UV irradiation at pH 12. This is a very indirect measurement of pyrimidine dimers- in contrast, the work described in this dissertation employs

direct chromatographic quantitation of pyrimidine dimers. In addition, Zavilgelsky and coworkers (1984) reported differences between high and low intensity irradiation based not on the dose delivered, but on the amount of damage sustained by the sample; points compared were not irradiated to the same fluence (dose), but to the same level of total degradation of the sample.

In this dissertation, I will discuss research that extended and improved the knowledge gained in the work described above. In my research, I used conditions approaching those of interest to biologists; I irradiated salmon sperm and plasmid DNA in aqueous solution at room temperature. I investigated various forms of UV light-induced DNA damage. I used a KrF excimer laser to deliver UV light at 248 nm at several different intensities, ranging from low ($3.15 \times 10^7 \text{ W/m}^2$) through intermediate (10^9 W/m^2 and 10^{10} W/m^2) to high intensity ($1.25 \times 10^{11} \text{ W/m}^2$). A wide range of comparable doses were delivered at all intensities investigated.

To determine the extent of damage inflicted by UV irradiation, I measured the extent of pyrimidine dimer formation directly. In addition to quantitating the extent of thymine-thymine dimer formation, I also directly measured the formation of thymine-cytosine dimers and of bimolecular

pyrimidine photoadducts. High intensity damage to DNA involving these species was not previously measured. At high intensity, formation of bimolecular pyrimidine photoproducts, characteristic of one-photon processes, is diminished. Rubin et al. (1981) reported that the triplet state of thymine was involved in the degradation of thymine through multi-photon processes following high intensity UV irradiation. Zavilgelsky et al. (1984), on the other hand, report that such degradation (and subsequent decrease in dimer formation) is not seen following irradiation with a nanosecond pulse laser, but only after irradiation with a picosecond pulse laser; this implies that only short-lived singlet states are involved in such damage. My experiments suggest that a significant fraction of bimolecular pyrimidine photoproducts (T^*T and T^*C cyclobutane dimers and $T(6-4)C$ photoadducts, see **DNA Photoproducts**) occur at conventional UV intensities via long-lived excited state intermediates. As discussed in this dissertation, my work reconciles prior results, and thus provides some insights regarding single-photon and biphotonic processes in DNA.

Additional experiments investigated the effects of high intensity laser irradiation on DNA strand breakage. Equivalent doses at increasing intensities were used, allowing one to separately consider the effects of dose and intensity.

Different effects were seen at different intensities. At high intensity there was an increase in the amount of strand breakage compared with that observed at low intensity. In addition, an event previously described only at extremely high doses (at conventional intensity) occurred frequently at low doses at high intensity: apparent double-stranded breakage, or the occurrence of two single-stranded breaks that are non-randomly opposed. Single- and double-stranded breaks are rare at conventional intensities of UV irradiation, and their occurrence at high intensity is reminiscent of the types of damage caused in DNA by ionizing irradiation (X-rays and gamma radiation). An independent mathematical model was developed from theoretical principles to analyze my experimental data regarding strand breakage. Curve fitting of my experimental data, as well as that of others, to the model confirms my suggestions regarding DSB's and SSB's.

In summary, I have shown that multi-photon events cause a decrease in the number of bimolecular pyrimidine photoproducts made in the DNA, and an increase in the amount of base damage and strand break damage sustained by the DNA. The current work shows that the damage incurred by DNA following irradiation is dependent not only on the total dose delivered, but also critically dependent on the rate (intensity) at which it is delivered. Indeed, while

increasing doses lead to increasing DNA damage, such increases in damage tend to be linear in nature. Damage due to increasing intensity, on the other hand, shows a second order dependence on intensity (as expected for an increasing frequency of biphotonic events), producing qualitative, as well as quantitative, differences in damage sustained by DNA.

My work has clear implications for the photochemistry of UV light damage to DNA at conventional intensities (on the order of 10 W/m^2), where single photon processes predominate. Specifically, it now appears that a large fraction of DNA damage arises via the lowest triplet excited state, or through long lived excimeric singlet states. Solar UV is an important environmental mutagen, the most important source of UV light at conventional intensities, and perhaps one of the most important sources of the early genetic variation necessary for evolution. Today, solar UV light is an important etiologic agent in the development of skin cancer in humans. The importance of UV damage to DNA can be seen in the increased incidence of such cancers in patient with congenital biochemical defects in UV damage repair pathways. Understanding the photochemical pathways that lead to UV-induced DNA damage may lead to therapeutic techniques that decrease such UV-induced damage to DNA. For instance, a range of harmless substances (including oxygen) have DNA triplet

state quenching properties, and could be exploited for such therapy. This work also may have some other implications for medicine, where it has been shown that UV lasers are useful surgical tools for various applications, most prominently for corneal surgery. My work demonstrating the level and nature of DNA damage induced by such lasers can help in developing the intelligent application of this technology. In summary, the current work helps us understand some previously hidden details of how DNA is damaged by UV light.

Excited States

Absorption of a photon by a molecule results in the deposition of energy, manifested as a promotion of an electron from a ground state orbital to a higher orbital. Such a molecule is said to be excited, or in an electronic excited state. The absorption of photons by molecules and the subsequent fate of those molecules is the province of spectroscopy and photochemistry (the former investigates the actual interactions between light and matter, the latter is concerned with light-induced chemical reactions). As much of this dissertation investigates the photochemistry of DNA, I will briefly review the generation and disposition of the excited states of molecules.

The exact description of the interaction between a photon and a molecule can be quite complex. If the molecule is as complicated as DNA, such interactions are only partially understood. Consequently, this discussion will focus on major principles. (More detailed information can be found in Moore (1962), Weidner and Sells (1968), Pesce (1971), or Häder and Tevini (1987), from which some of this discussion is derived.) Usually, there are as many electrons as protons in an atom, and the electrons are thought of as occupying orbitals around

the atomic nucleus. The position of any one electron in a particular orbital can be described by a wave function that predicts where the electron can most probably be found. The Heisenberg uncertainty principle (Moore, 1962; Weidner and Sells, 1968) tells us that it is impossible to know exactly where the electron will be. Orbitals are usually drawn in diagrams as clouds of electric charge that surround the atomic nucleus; these clouds typically are drawn to show where an electron in that orbital can be found about 95% of the time. There is a specific arrangement of orbitals around the atomic nucleus. Electrons in each succeeding orbital are found, on average, further and further away from the nucleus. The outer orbitals are often called higher orbitals (when compared with those closer in) because they contain electrons with higher energies. As the electron's distance from the nucleus increases, so does the energy of the electron. Electrons in some atoms and molecules may be so far away from the nucleus and be so energetic that they are barely held in orbit. These electrons have energies that approach the ionization limit (that is, the electron may depart from the orbital, leaving behind an ion or ion-radical). Usually, electrons are arranged so that the energy of the atom is minimized, that is, the electrons tend to be close to the atomic nucleus. Not all

possible orbitals are therefore filled. This condition is known as the ground state.

Each electron can be assigned a quantum number that describes which orbital the electron inhabits. Each electron, in addition to spinning around the atomic nucleus, also spins around its own axis. This spin also contributes to the quantum number of the electron; by definition, the two possible spin directions for an electron are $+1/2$ and $-1/2$. According to the Pauli exclusion principle (Moore, 1962), no two electrons in an atom can have the same quantum number, but two electrons can differ by only their spin number. This means that a maximum of two electrons can occupy any one orbital; if there are two electrons in an orbital, they have, by definition, opposite spins. A consequence of the arrangement of electrons around the atomic nucleus is that electrons must occupy discrete orbitals, each of which has a distinct energy level associated with it.

This arrangement of electrons into discrete orbitals with distinct energies becomes important when atoms or molecules interact with photons. If a photon is absorbed by an atom or molecule, the energy of the photon is manifested by an outer electron being boosted to a higher orbital (Figure 1). To move to the higher orbital, the energy of the photon absorbed by the atom or molecule must correspond closely to the energy

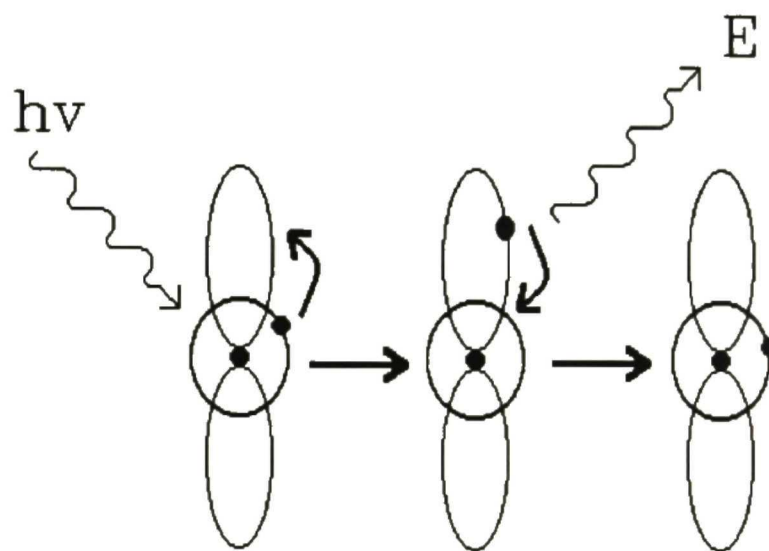


Figure 1- Schematic Diagram of Atomic Excitation. In the first drawing, a photon, $h\nu$, interacts with a simple atom; the energy of the photon is absorbed, elevating an electron from the less energetic ground-state orbital (single-circular orbit) to a more energetic orbit further from the nucleus (double-circular orbit, middle drawing). Relaxation, or return to the ground state, is accompanied by a release of energy, E (last drawing).

difference between the lower and higher orbital. This means that only photons with energies comparable to the spacing between orbitals can excite atoms or molecules, that is be absorbed by them. Since electrons can not fit between orbitals, photons with intermediate energies are not absorbed. The energy spacing between excited states is not constant, but decreases as the energy of the higher orbitals increases. Therefore, the more energetic excited states tend to be closer together, up to the ionization limit of the atom or molecule. If a molecule should absorb a photon with sufficient energy to exceed the ionization limit, an outer electron becomes sufficiently distant from the nucleus to become a free electron, leaving behind a positive ion or ion-radical.

Electrons in DNA are most typically excited by UV light to the first (lowest) excited state above the ground state. The energies needed to reach excited states above the first excited state ($>S_1$) correspond to photons of very short wavelengths, those in the vacuum UV or proximal X-ray region of the electromagnetic spectrum (wavelengths less than 100 nm). Visible light is sufficient to excite molecules containing unpaired electrons to S_1 , while molecules containing paired electrons in stable orbits need the greater energy characteristic of ultraviolet light for promotion to S_1 . It is possible that an excited molecule will absorb a

second photon of appropriate wavelength, and receive additional energy. Such a molecule would then move from the first (S_1) to the second (S_2), or even to an higher excited state. In practice, though, the lifetime of the singlet excited state is so short that it is very unlikely it will encounter a second photon before it returns by one of various means to the ground state.

Two paired electrons normally have opposite spins. This is known as the singlet state, a term derived from the electron pair's multiplicity M , defined as $M=2|S|+1$, where S is the spin quantum number (Moore, 1962; Häder and Tevini, 1987). (The multiplicity (M) is a term derived from the Schrödinger wave functions used to describe an atom.) With two paired electrons spinning in opposite directions, $S=+1/2$ for one electron and $S=-1/2$ for the other, so $M=2|1/2-1/2|+1=1$, and the atom or molecule is referred to as being in the singlet state (Figure 2). Typically, the lowest singlet state, S_0 , is identical to the ground state, G_0 . If a molecule absorbs a photon, the photon's energy is manifested as an electron being boosted to a higher orbital. Should this happen, the multiplicity M remains 1, as the boosted electron continues spinning in the same direction; the molecule is said to be in a singlet excited state, typically in the lowest singlet excited state, S_1 . Since the spin of the electron is

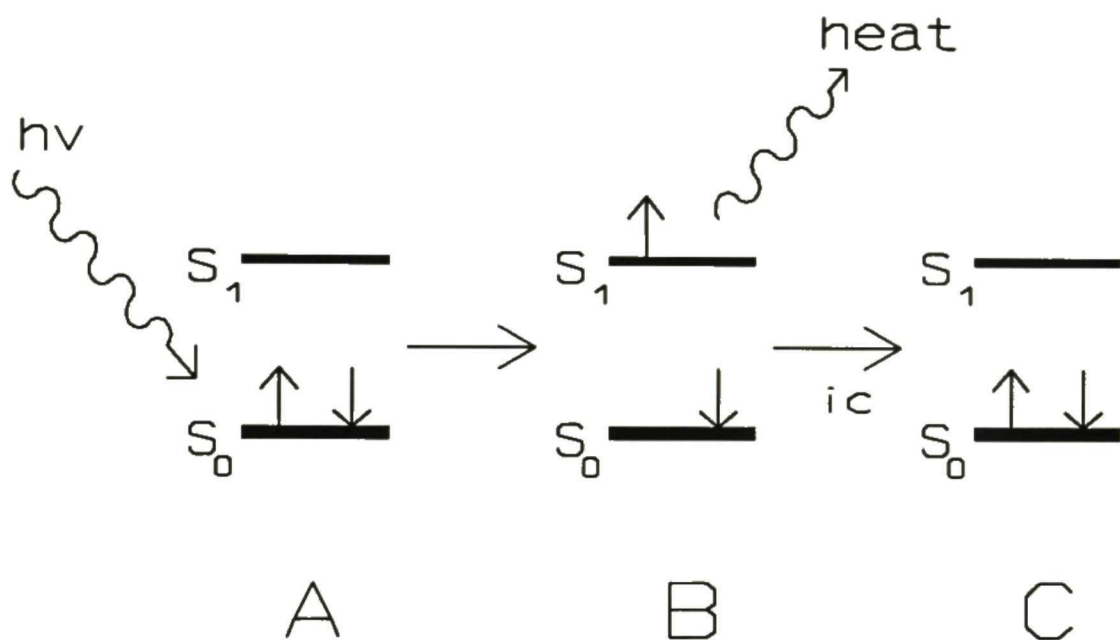


Figure 2- The Singlet Excited State: **A-** Two electrons with opposite spins in the ground state orbital of an atom (up and down arrows on S_0) interact with a photon ($h\nu$). **B-** Absorption of the photon's energy results in promotion of the atom to the first singlet excited state (S_1), manifested by elevation of an electron to a more energetic orbital, without changing the spin of the electron. **C-** Relaxation by internal conversion (ic) with release of heat results in the return to the ground state. Other modes of decay are also possible.

unchanged, it can readily decay to the ground state, to occupy its previous orbital. The half life of the first singlet excited state is correspondingly short, on the order of picoseconds for aqueous DNA at room temperature.

An alternate mode of decay is possible, however, in which the boosted electron reverses its spin while remaining in the excited state orbital. In this case, the energy of the molecule is reduced, but not fully reduced to the ground state. The spin of the excited electron and that of its former partner are now the same, and the multiplicity $M=2|1/2+1/2|+1=3$ or $M=2|-1/2-1/2|+1=3$; the multiplicity $M=3$ and the excited molecule is said to be in the triplet excited state, T_1 (Figure 3). T_1 tends to be much longer lived than S_1 , because the electron must once again reverse its spin to return to the ground state. The Pauli exclusion principle tells us that the boosted electron cannot return to the same orbital as its former partner, for then it would have the same spin as its partner, which is disallowed. Such a transition is referred to as "forbidden". The simultaneous reversal in spin and demotion of the highest lying electron producing the transition from T_1 to S_0 (or the equivalent G_0) occurs rarely as compared to the S_1 to S_0 transition. While the latter transition (S_1 to S_0) occurs within picoseconds in DNA, the

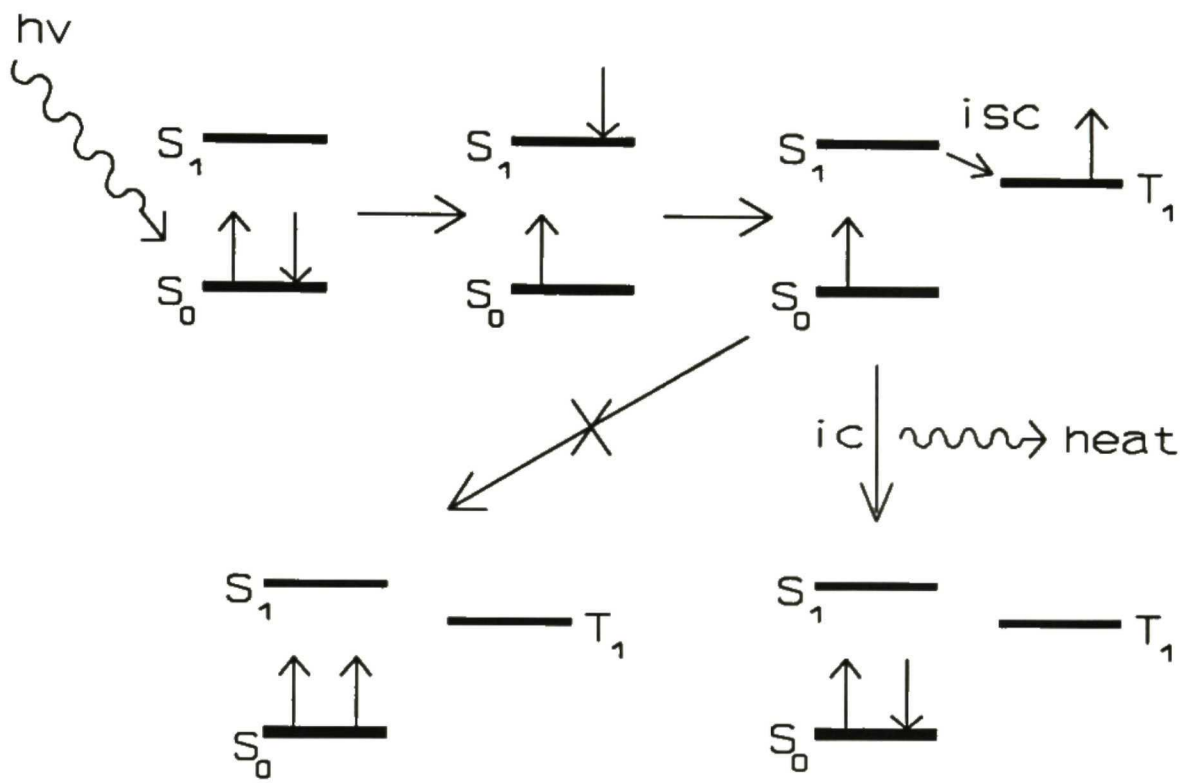


Figure 3- The Triplet Excited State. Two electrons with opposite spins in the ground state orbital of an atom (up and down arrows on S_0) interact with a photon ($h\nu$). Absorption of the photon's energy results in an increase in the atom's energy and promotion to the first singlet excited state (S_1), followed by partial relaxation through spin reversal, that is intersystem crossing (isc) to the first triplet excited state (T_1). Relaxation to the ground state occurs through spin reversal and internal conversion (ic) with release of heat. Other modes of decay are also possible; decay without spin reversal does not occur (Pauli exclusion principle; shown as two up arrows in bottom left panel).

excited state lifetime of T_1 prior to return to S_0 is very much longer, on the order of microseconds.

Direct transitions from the ground state to triplet excited states do not occur; instead, the triplet state is attained via the S_0 to S_1 transition, followed by "intersystem crossing", the reversal of electron spin producing the triplet state. This is a mode of decay, as T_1 is less energetic than S_1 , and occurs with an efficiency of 1.23% for thymine in aqueous solution at room temperature (Fisher and Johns, 1970).

Once an atom or molecule has been excited, it returns to the ground state. In doing so, it must release the energy it acquired from the photon. This return to the ground state with release of energy is known as relaxation, and can occur by a variety of paths (Figure 4). As noted above, relaxation from S_1 to S_0 in DNA in aqueous solution at room temperature is usually very rapid, with a half life of picoseconds (10^{-12} s). Usually this decay occurs via the release of heat, a process known as internal conversion. An alternate release of energy can occur by the emission of a photon. The energy absorbed by the atom or molecule from a photon is released in the atom's or molecule's subsequent relaxation as a second photon. This process is known as fluorescence, and is studied by spectroscopists, who can determine energy levels and investigate chemical reactions by analyzing such emitted

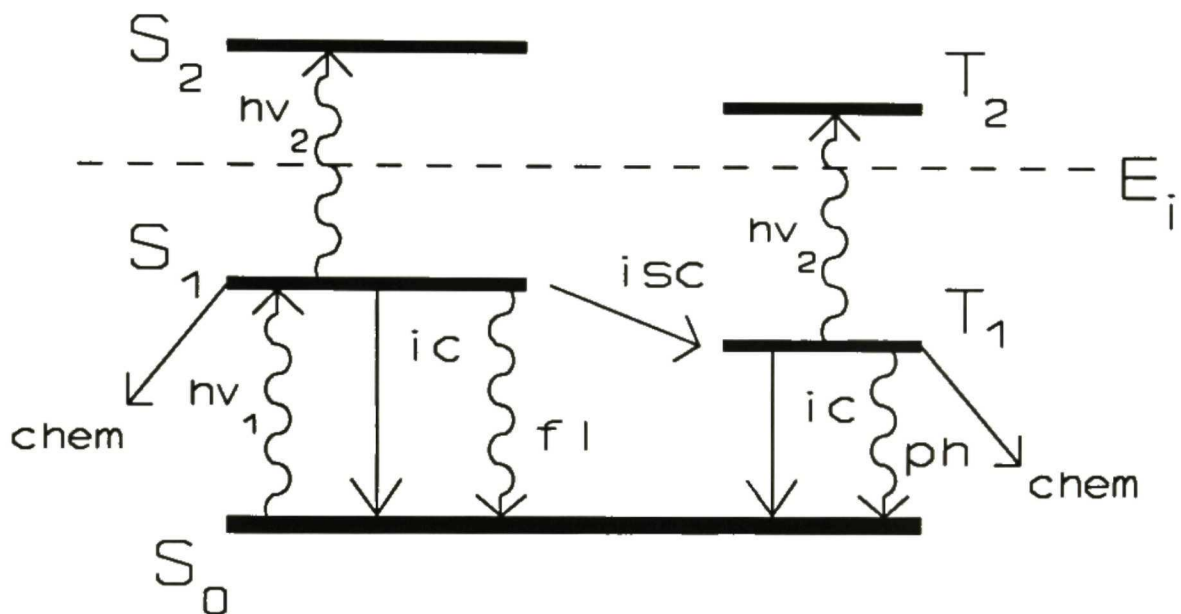


Figure 4- Schematic of Relaxation Modes. Schematic diagram of changes in energy of an atom or molecule following absorption of a photon; energy increases from bottom to top in this diagram. $h\nu_1$, $h\nu_2$ -first and second absorbed photon; isc -intersystem crossing; ic - internal conversion; fl -fluorescence; ph - phosphorescence; $chem$ - participation in a chemical reaction; S_0 - ground state; S_1 , S_2 - first and second (or higher) singlet excited states; T_1 , T_2 - first and second (or higher) triplet excited states; E_i - ionization energy.

photons. The energy of the emitted photon cannot be greater than that of the exciting photon; thus the emitted photon has a longer wavelength than the exciting photon.

Under appropriate conditions, the energy of the S_1 state is used for alteration of covalent bonds, either within the excited moiety itself, or in conjunction with other unexcited moieties. This latter process requires that a suitable target for reaction be present in the vicinity of the excited molecule within the picosecond or so lifetime of the S_1 state. Finally, as described above, S_1 can undergo intersystem crossing to the less energetic first triplet excited state, T_1 .

Relaxation from the triplet state occurs via pathways similar to relaxation from the singlet state. Most triplet states decay to the ground state within microseconds through internal conversion, losing energy as heat. Because of their long excited state lifetimes, triplet state atoms or molecules are often involved in chemical reactions, and return to the ground state by recombination with other molecules. The triplet state can also decay to the ground state by emitting a photon, a process known as phosphorescence. As with fluorescence, the wavelength of the emitted photon is longer than that of the exciting photon. Because the lifetime of the triplet state is much longer than that of the singlet state,

phosphorescence tends to occur much later than fluorescence, and appropriate compounds can be observed emitting photons seconds to hours after the source of exciting photons is removed. The most common method of relaxation from either the singlet or triplet state is through internal conversion, or through the emission of photons as fluorescence or phosphorescence.

In general, a single photon will interact with and excite a single atom or molecule. However, under certain conditions, more than one atom or molecule can be effectively excited by one photon. This occurs most easily in molecules that have planar ring structures and a series of conjugated double bonds. In such molecules (benzene is an example), the p-orbitals of the constituent atoms overlap, creating double bonds; the electrons are then essentially shared by the atoms joined by the double bond, and travel in π -molecular orbitals. Because the molecule is planar, there is considerable overlap of π -orbitals across the entire ring structure; electrons become delocalized, and participate in the π -orbitals between several atoms. In sufficiently concentrated solutions of such molecules, it is possible that two molecules can be in close proximity when one of the molecules absorbs a photon. The energy of the photon may then become de-localized over both

molecules, leading to an excited state that involves two molecules. This excited state is more stable than the more usual uni-molecular or single atom excited state. Such an excited-state dimer is known as an excimer. In DNA, both purine and pyrimidine bases have planar ring structures that include double bonds; additionally, the bases are held fairly rigidly in a face-to-face orientation, in close proximity. It is conceivable that excimers may form readily in DNA following the absorption of a photon. The existence of such excimers has been inferred from fluorescence spectroscopy of calf thymus DNA, poly(dA-dT), and nucleosides following UV light excitation (Ballini et al., 1983; Rigler et al., 1985; see Discussion for details).

DNA PHOTOPRODUCTS

The photochemistry of DNA and its constituents following UV irradiation at conventional intensities has been well studied (see, for example, Wang, 1976b). The vast majority of this work was carried out using simple equipment. A GE germicidal lamp is a convenient source of low intensity UV light (254 nm, intensities up to about 10 W/m^2), and equipment used to determine dosimetry is readily available.

There are many forms of damage to DNA following UV irradiation, but only a few are investigated in this work (Figure 5). My work is concerned with bimolecular pyrimidine photoproducts and with the cleavage of covalent bonds, both of the glycosylic bond between the sugar and the base of the DNA, and of bonds in the sugar phosphate backbone. Bimolecular pyrimidine photoproducts investigated include the pyrimidine dimers and pyrimidine photoadducts.

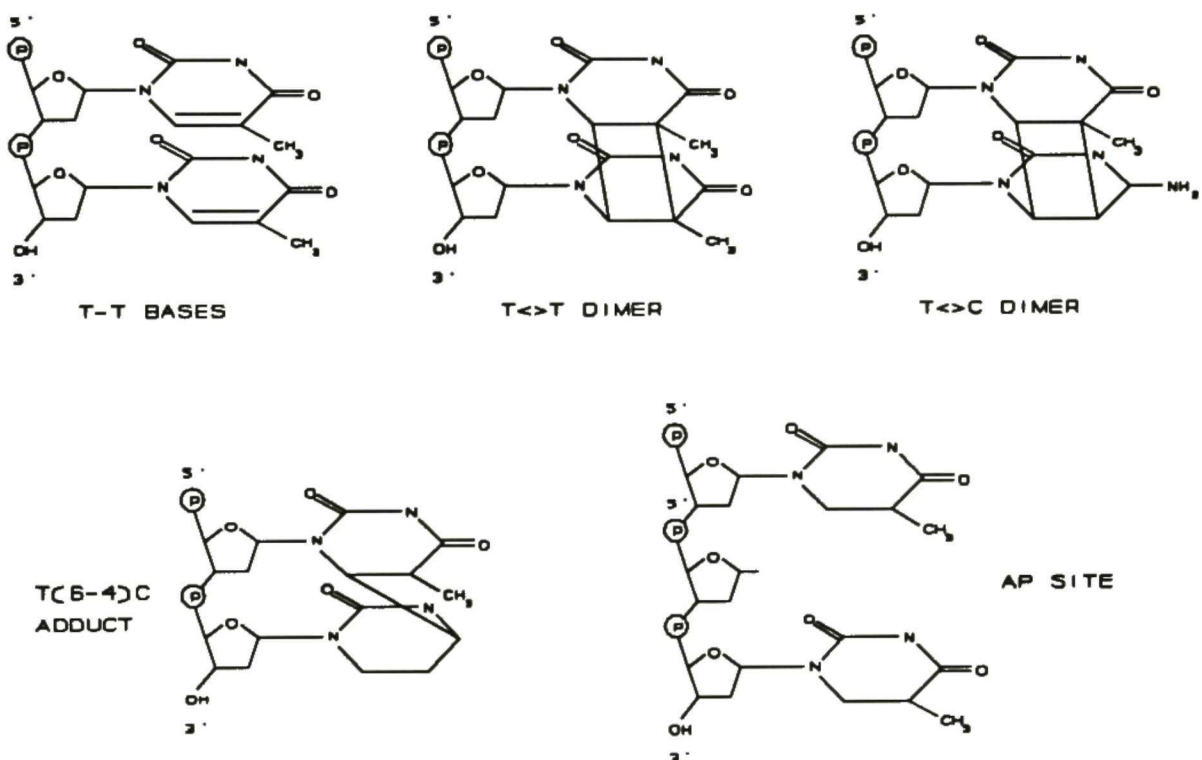


Figure 5- The Major DNA Photoproducts

The most common pyrimidine photoproducts seen after UV irradiation is the thymine dimer (T^T). The thymine dimer is formed when two adjacent thymines become joined, concomitant with the saturation of the 5,6 double bonds of thymines involved (Fisher and Johns, 1976). This results in the formation of a cyclobutane ring between the 5 and 6 positions of the adjacent thymines, joining them together (Figure 5). The T^T dimer is formed in DNA with an efficiency (quantum yield) of about 0.02 (Patrick and Rahn, 1976; Patrick, 1977), though under appropriate conditions nearly all theoretically possible T^T dimers in DNA can be made (using triplet sensitization, see Discussion). The thymine dimer is stable to formic or trifluoro-acetic acid and heat, allowing one to separate the dimer from monomeric DNA bases following degradation of the glycosilic bonds in DNA by acid hydrolysis (Patrick and Rahn, 1976).

Following increasing doses of UV light, one sees an increase in dimer content of DNA, up to a point. After a certain level of dimers is reached, a plateau value is established- increasing the dose does not increase the number of dimers seen. This is due to the fact that UV light not only creates dimers from monomers, but also reverses dimers to monomers. This photolysis is more pronounced at shorter wavelengths (~240 nm), whereas dimer formation predominates

at longer UV wavelengths (~280 nm) (Fisher and Johns, 1976; Patrick and Rahn, 1976). Thus if one irradiates DNA with long wavelength UV light, one sees a greater plateau level of dimer formation than if one uses a shorter wavelength of UV light. Dimers between adjacent thymines and cytosines also exist; these T^C dimers are similar to T^T dimers, except they are made with one-tenth the efficiency (quantum yield about 0.002) (Patrick and Rahn, 1976; Patrick, 1977).

The second class of photoproducts I investigated is the pyrimidine 6-4 photoadduct (Figure 5). This is a pyrimidine dimer (adduct) that is created when two adjacent pyrimidines become joined between the 6 position of the 5' base and the 4 position of the 3' base, involving the saturation of the 5,6 double bond of the 5' base. The most common of these photoproducts is an adduct of a 5' thymine and a 3' cytosine: T(6-4)C or 6-4'-(pyrimidin-2'-one)thymine. Unlike the cyclobutane dimers, T(6-4)C is not lysed by UV light in the 240-280 nm range (Patrick and Rahn, 1976), and adduct levels tend to increase as UV dose increases (Franklin et al., 1982). T(6-4)C adducts are stable to hot trifluoro-acetic acid (but not formic acid), and can be isolated from monomeric bases by acid hydrolysis of DNA. The quantum yield for T(6-4)C lesions is quite low, estimated at 0.0015 (Patrick and Rahn, 1976; Patrick, 1977).

If a DNA base is severely damaged (by UV or ionizing radiation), it may undergo cleavage of the glycosylic bond between the sugar and the base. If this occurs, the base is freed from the DNA backbone, and an apurinic or apyrimidinic site (AP site, Figure 5) is created. While AP sites were not directly assayed in my work, release of bases from DNA was. Experiments examining the release of free bases indicated the existence of many AP sites, which may cause local denaturation of the DNA, and lead to further damage, such as the induction of strand-breaks.

Strand breaks, both single-stranded (SSB's) and double-stranded (DSB's), are seen following exposure of DNA to ionizing radiation (X-rays and γ -rays) (Cerutti, 1976). Such strand breaks are biologically important, and in the case of double-stranded breaks, believed to be highly lethal lesions in low number (van der Schans et al., 1973). When DNA is irradiated in aqueous solution with X-rays or γ -rays, the ionizing radiation creates water-derived radicals, such as the hydroxyl radical. Reaction of the hydroxyl radical with the sugar moiety of the DNA backbone leads to the generation of strand breaks (von Sonntag et al., 1981). Water derived radicals also react with DNA bases, leading to a wide variety of base damage, including ring opening and fragmentation

(Scholes, 1976). Strand breaks and base damage are also observed following irradiation of dry DNA and following induction of free radicals in solid pyrimidine bases (Scholes, 1976; von Sonntag *et al.*, 1981). Under these conditions, damage is not due to reaction with water derived radicals, but must involve the formation of radical species within the DNA bases themselves. It is believed that ionizing radiation damage to DNA *in vivo* occurs both directly (by direct interaction of photons or particle radiation with DNA), and indirectly, through water derived radicals. Biphotonic excitation of DNA by UV light, therefore, serves as a model of the direct form of DNA damage induced by ionizing radiation (Opitz and Schulte-Frohlinde, 1987; Bothe *et al.*, 1990).

MATERIALS AND METHODS

Preparation of DNA Samples.

a) Salmon Sperm DNA. Salmon sperm DNA was purchased from Sigma, and labeled by nick translation with [*methyl*-³H]TTP. Labeled DNA was purified on a Sephadex G75 column (5 ml) and dialyzed extensively against TE (10 mM Tris-HCl, pH 8, 1 mM EDTA) to remove any unincorporated label (Maniatis *et al.*, 1982; Ausbel *et al.*, 1989). The specific activity was 8 x 10⁶ cpm/μg.

b) Plasmid DNA. pUC19 plasmid DNA was purified by a modified Triton X-100/lysozyme lysis procedure (Maniatis *et al.*, 1982; Ausbel *et al.*, 1989). Briefly, *E. coli* strain DH5α containing pUC19 plasmid was grown overnight, and inoculated into one liter of enriched "terrific" broth (12 gm tryptone, 24 gm yeast extract, 12.5 gm K₂HPO₄, 2.3 gm KH₂PO₄, 4 ml 100% glycerol per liter) (Micheal D. Smith, personal communications). After overnight growth, cells were pelleted, washed, and resuspended in freshly made 25% sucrose, 50 mM Tris-HCl (pH 8), 1 mM EDTA, 50 mg/ml lysozyme. After incubation for 1/2 hour, cells were

lysed by the addition of 0.4% Triton X-100, 60 mM EDTA, 0.1 M Tris-HCl (pH 8); cell debris and chromosomal DNA were pelleted by centrifugation in a Sorvall SS34 rotor at 19k rpm for 45 minutes. Supernatant containing plasmid DNA was collected; plasmid DNA was purified by isopycnic centrifugation in CsCl/ethidium bromide. Further purification was accomplished by a second round of centrifugation in CsCl/ethidium bromide. Purified supercoiled plasmid DNA was collected, ethidium bromide was removed by extraction with CsCl saturated *n*-butanol, and DNA was desalted by dilution (addition of 2.5 volumes distilled water), and ethanol precipitated.

c) M13 RF DNA. M13mp7 and M13mp18 replicative form (RF) DNA was purified by a procedure similar to the one used for pUC19. A 1/10 dilution of an overnight culture of *E. coli* strain JM103 was grown in one liter broth until it reached an absorbance of $A_{600}=0.5$. 500 μ l of M13 phage stock (containing 10^{10} to 10^{11} pfu/ml) was added to the culture. After one hour incubation, chloramphenicol was added to a final concentration of 170 μ g/ml, and the cells were incubated for an additional four hours. The cells were then pelleted, washed, and DNA was

purified as described above (Maniatis et al., 1982; Ausbel et al., 1989; Micheal D. Smith, personal communications).

Laser Irradiation.

Samples were irradiated with a Questek model 2640 KrF excimer laser. The laser emits 20 ns pulses at a wavelength of 248 nm. Four intensities were ultimately employed- $1.25 \times 10^{11} \text{ W/m}^2$, $1.16 \times 10^{10} \text{ W/m}^2$, $2.5 \times 10^9 \text{ W/m}^2$, and $3.15 \times 10^7 \text{ W/m}^2$ (average intensity for the duration of the laser pulse). In all cases the beam was focused with a 350 mm fused silica plano-convex lens placed 45 mm from the laser, and the sample was placed beyond the focal point; this provided a divergent beam that evenly illuminated the entire sample. The highest intensity was achieved by placing the sample in the unattenuated laser beam approximately 630 mm from the laser; the next highest intensity was attained by placing the sample in the unattenuated beam approximately 1200 mm from the laser. For the second lowest intensity and lowest intensity, one or two beam splitters (99% reflectance, 1% transmission), respectively, were placed in the beam path before the sample, which was placed approximately 700 mm from the laser (Figure 6). Thermoelectric dosimetry (Questek, Laser Precision

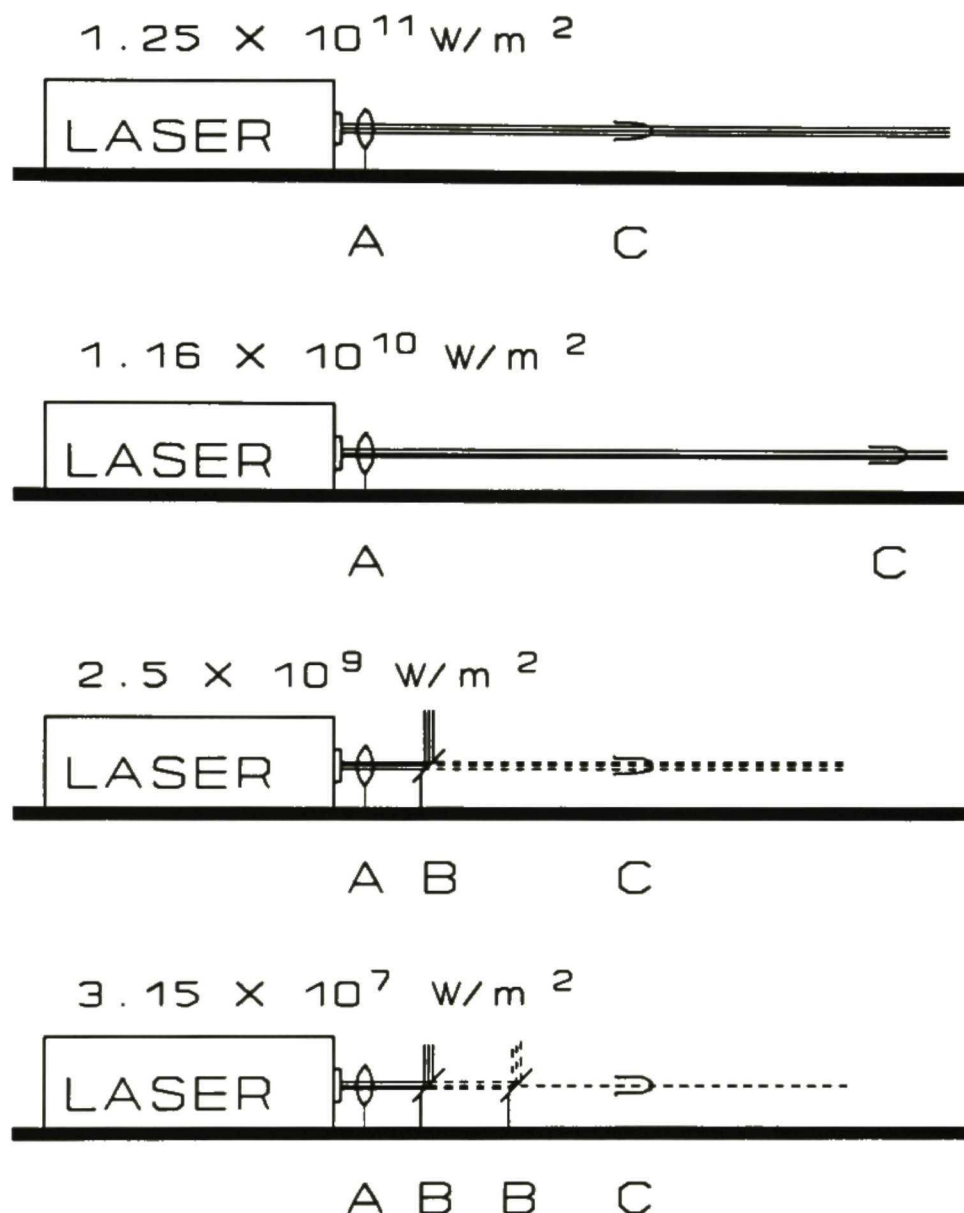


Figure 6- Laser Set-Up. This diagram shows how the laser was set up to achieve irradiation at the four intensities indicated. **A**- plano-convex, fused silica lens (focal length 350 mm); **B**- beam splitter (99% reflectance, 1% transmission at 248 nm) placed at 45° to the beam path; **C**- DNA sample in an Eppendorf tube placed horizontally in the beam path.

Corporation) was employed to measure beam intensity and fluence during each experiment. The laser beam was monitored with a diode matrix (from Spiricon), a thermoelectric device (from Laser Precision Corporation), and a digital oscilloscope (Tektronix). Early experiments found that the beam closely approximated a square wave for the duration of the pulse, and internal laser optics were adjusted to insure uniform intensity throughout the beam cross-section.

Six doses (0, 2500, 5000, 10000, 20000, 30000 J/m²) were delivered at four intensities (10^7 , 10^9 , 10^{10} , and 10^{11} W/m²). At each dose, the total number of photons incident upon the sample was the same, regardless of intensity, but the time over which the samples were irradiated decreased with increasing intensity. For example, only one 20 ns pulse was required to achieve a dose of 2500 J/m² at the highest intensity (1.25×10^{11} W/m², 2500 J/m²/pulse); at the lowest intensity (3.15×10^7 W/m², 0.63 J/m²/pulse), 3968 pulses, each 20 ns long, were delivered over 1.3 minutes at a rate of 50 pulses per second. By delivering equivalent doses at four different intensities, the effects of dose (number of photons delivered to the sample) and intensity (rate at which photons were delivered to the sample) could be evaluated separately.

Irradiated Samples.

For experiments in which bipyrimidine photoproducts were determined, 250 ng of radio-labeled salmon sperm DNA in 50 μ l distilled water was placed at the bottom of a 1.5 ml Eppendorf tube (sample depth 4 mm), that was held horizontally in the beam path beyond the focus, as described above. For DNA strand breakage experiments, 5 μ g of supercoiled plasmid DNA or M13 RF DNA was irradiated in 50 μ l of either distilled water or 100 mM NaCl. Samples were placed at the bottom of 1.5 ml Eppendorf tubes (sample depth 4 mm), and were mounted horizontally for the irradiation. In all cases, samples were gently mixed at intervals during the irradiation to insure that all of the sample was evenly and equally illuminated.

Analysis of DNA Dimers.

Following irradiation, salmon sperm DNA samples (radiolabelled with $[\text{methyl-}^3\text{H}]$ thymine) were ethanol precipitated, resuspended in 5 μ l trifluoroacetic acid (TFA), and hydrolyzed at 180°C for 90 minutes (Figure 7). Hydrolysates were spotted on Whatman No.3 paper, and developed by descending

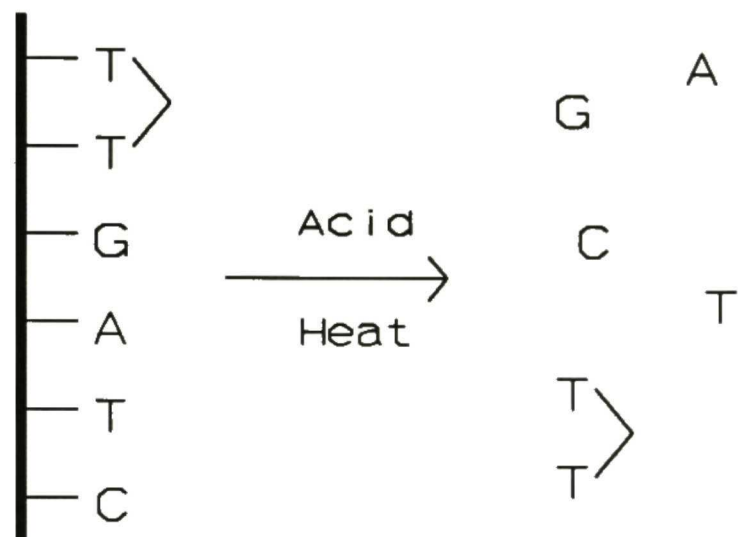


Figure 7- Acid Hydrolysis of DNA. This schematic shows the fate of DNA and its constituents following acid hydrolysis. The DNA backbone (thick line) is degraded, and the monomeric and dimeric DNA bases that remain can be chromatographically separated.

chromatography for 8 inches using *n*-butanol/acetic acid/water (80:12:30, by volume). The resulting chromatogram was cut into 1/4 inch fractions and each fraction was eluted into water overnight with continuous gentle shaking. The level of radioactivity in each fraction was then determined by scintillation counting. This method of chromatography separates T³C and T³T dimers from each other, and from DNA base monomers, which migrate more rapidly than the dimers. Pyrimidine photoadducts {T(6-4)C} co-migrate with T³T dimers in this system, and must be separated by additional chromatography. This was accomplished by pooling eluates from the fractions of the first chromatogram that contained the T³T and T(6-4)C products (both in one peak), spotting them on Whatman No.3 paper, and developing for 8 inches with a second solvent, *t*-butanol/methyl ethyl ketone/water/58% ammonium hydroxide (4:3:2:1, by volume). After development, 1/4 inch fractions were cut and scintillation counted, and thus amounts of T³T and T(6-4)C determined. Markers for all chromatography were derived from salmon sperm DNA labeled in thymine by nick-translation and irradiated at 254 nm with a GE germicidal lamp. The R_f values for all markers and photoproducts derived from laser irradiation closely matched those of the published values for these photoproducts (Varghese and Wang, 1967; Nguyen and Minton, 1988).

Release of Thymine and Thymine Products from DNA.

Salmon sperm DNA, containing [*methyl-³H*]thymine, was irradiated in water (as described in **Irradiated Samples**), and samples were concentrated in a vacuum centrifuge and spotted on plastic-backed G60 silica gel thin layer chromatography (TLC) plates (Merck). The plates were developed with ethyl acetate/*n*-propanol buffer (4:1, by volume, water saturated). After chromatography, the plates were dried, and the silica was gently removed from the plates by the "Scotch tape" method. This method involves the application of transparent tape (3M) to the plate, and careful removal of the tape with adherent silica gel material. When done with care, essentially all the silica material adheres to the tape, and can be completely stripped from the plastic backing plate when the tape is removed. The tape was cut into thirty-six equal fractions, and the level of radioactivity in each fraction was determined by scintillation counting. In this system, bases, nucleosides, and fragments thereof travel with characteristic mobilities, while phosphate containing groups (such as nucleotides or DNA) remain at the origin (Masnyk et al., 1989; Menshonkova et al., 1980).

Analysis of DNA Strand Breakage.

Strand breakage was analyzed by alterations of plasmid and M13 RF (double stranded) DNA conformations. Supercoiled plasmid and M13 RF DNA was used, as changes in the conformation of supercoiled DNA reflect the accumulation of strand breaks. Form I (supercoiled), Form II (open circular), and Form III (linear) DNA were separated by gel electrophoresis. Immediately after irradiation of supercoiled M13 RF or plasmid DNA, samples were diluted with an equal volume of loading buffer (30% glycerol, 0.25% bromophenol blue, 0.25% xylene cyanol), and aliquots were loaded in agarose gels for electrophoresis. 1 μ g DNA was loaded per lane, one lane per sample. Electrophoresis quality agarose (UltraPure, Bethesda Research Laboratories) was used at a concentration of 1.5% (for M13 samples) or 2% (for pUC19 samples). TEA (40 mM Tris-acetate (pH 8), 1 mM EDTA) was used as the running buffer. Gels were run at 50 volts (2.5 V/cm) for 9 hours. After electrophoresis, they were stained for one hour in ethidium bromide (0.4 μ g/ml), and destained for 45 minutes in distilled water.

Densitometry.

After staining and destaining, gels were photographed by transillumination (Fotodyne Foto-UV transilluminator) using Polaroid Type 55 film. Positive prints were coated and saved, and negatives were fixed for two hours in 18% sodium sulfite (Sigma), washed for several hours in water, and dried. After drying, negatives were mounted on a glass plate and densitometrically scanned (Hoefer Scientific Instruments model GS300 transmittance/reflectance Scanning Densitometer; Shimadzu CS-910 Dual Wavelength TLC Scanner). Areas under peaks were integrated using a Shimadzu model C-R1B Chromatopac integrator, and were used to determine relative amounts of DNA in Form I (supercoiled), Form II (open circle), and Form III (linear). The total amount of DNA in all three peaks (bands) for each irradiated sample was summed and compared to the amount of DNA in the control (unirradiated) lane; since equal amounts of DNA were loaded into each lane (1 μ g in each lane), it was assumed that DNA not present in Form I, II, or III peaks consisted of heterogenous linear fragments shorter than the length of the M13 or plasmid (termed "Form F"). By definition, then, Form F DNA is linear DNA of less-than unit length, one unit being equal to the length of a linear plasmid or M13 RF molecule.

Mathematical Modeling.

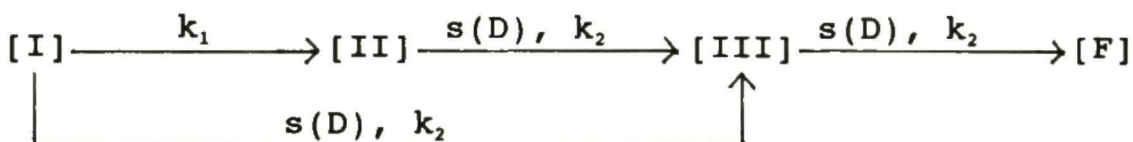
Densitometry data were analyzed with the mathematical modeling program MLAB, available on the National Institutes of Health DEC-10 computer (Division of Computer Research and Technology, NIH). Curve fitting was by minimization of sum of squares using the Marquardt-Levenberg method (Marquardt, 1963; Smith, 1970) and a quadratic algorithm for convergence within linear constraints (Schrager, 1972). Analytical functions describing the amounts of Forms I, II, III, and F present after irradiation of DNA were developed (see **Strand-break Functions**). These functions were fit to the experimental data obtained by densitometry, and single-strand break and double-strand break constants for dose dependence (k_1 and k_2 , respectively) at each given intensity were determined.

Strand-break Functions.

I derived expressions for the quantity of plasmid DNA in various forms following exposure to UV-irradiation. The following terms were employed: SSB is a single-stranded break produced by a single event; DSB is a double-stranded break produced by a single event; S is a scission produced by two

independently occurring SSB's on opposite strands, and sufficiently close to yield a double-stranded cleavage; and M is the sum of monomers in a piece of DNA, equal to the number of nucleotides. In double-stranded DNA, $M/2$ equals base-pairs.

In deriving the mathematical expressions, I used a schematic model describing the conversion of supercoiled plasmid DNA to various conformational forms as a function of UV exposure. The model which I developed is:



(scheme 1)

where I is Form I DNA (supercoiled); II is Form II DNA (open circular); III is Form III DNA (linear); F is plasmid DNA containing more than one DSB or S, yielding linear fragments shorter than Form III; k_1 is the dose-constant per monomer for formation of SSB (SSB/base/Jm⁻²); k_2 is the dose-constant per monomer for formation of DSB (DSB/base/Jm⁻²); D is dose, measured as Joules/meter² (J/m² or Jm⁻²); and $s(D)$ is a function of dose (D) for the yield of scissions (S). Scissions are a function of dose, unlike the dose-constants k_1 and k_2 , since the likelihood of an SSB resulting in S depends on the

frequency of SSB's already present, whereas formation of SSB's and DSB's do not.

Expressions for the number of SSB's and DSB's in a given DNA fragment are

$$SSB = k_1 MD + SSB_0 \quad (\text{eq. 1}),$$

$$DSB = k_2 MD + DSB_0 \quad (\text{eq. 2}),$$

where SSB_0 and DSB_0 are the numbers of SSB's and DSB's preexisting prior to UV irradiation. In the experiments under consideration the consequences of SSB_0 and DSB_0 are negligible. At initial conditions most plasmid is in Form I, indicating $SSB_0 = DSB_0 = 0$ for this species. One SSB converts Form I to Form II, and at initial conditions, Form I > Form II, thus SSB_0 in Form II is no more than a few per plasmid, and $DSB_0 = 0$. There is no Form III or Form F initially, and $SSB_0 = DSB_0 = 0$ for these species. Accordingly, to simplify expressions 1 and 2, SSB_0 - and DSB_0 -containing terms are eliminated. (Numerical simulations showed that this introduces no appreciable error.) Assuming the absence of Form III or Form F at initial conditions, Eqs. 1 and 2 become:

$$SSB = k_1 MD \quad (\text{eq. 3}),$$

$$DSB = k_2 MD \quad (\text{eq. 4}).$$

The expression for $s(D)$ is derived as follows. For a fragment of double-stranded DNA (Schumaker et al., 1956; Minton and Friedberg, 1974):

$$S = (M/2)(2B+1)P^2 \quad (\text{eq. 5}),$$

where S is the number of scissions per molecule of $M/2$ base-pairs; P is the probability that any given backbone bond is broken; B is the maximum number of nucleotides by which two SSB's on opposite strands can be staggered without preventing scission; and $M \gg 1$. Substituting $P = SSB/M$, and eq. 3 into eq. 5 yields:

$$S = k_1^2 D^2 M (2B+1)/2$$

$$\text{or} \quad s(D) = k_1^2 D (2B+1)/2 \quad (\text{eq. 6}),$$

where $S = s(D)DM$.

Dose laws developed from scheme 1 can be expressed as:

$$d[I]/dD = (-k_1 - k_2 - s(D))M[I] \quad (\text{eq. 7}),$$

$$d[II]/dD = k_1 M[I] - (k_2 + s(D)) M[II] \quad (\text{eq. 8}),$$

$$d[III]/dD = (k_2 + s(D)) M([I] + [II] - [III]) \quad (\text{eq. 9}),$$

and $d[F]/dD = (k_2 + s(D)) M[III] \quad (\text{eq. 10});$

their solutions are:

$$[I] = [I_0] e^{-k_1 MD - f(D)} \quad (\text{eq. 11}),$$

$$[II] = \frac{[II_0] + [I_0] (1 - e^{-k_1 MD - f(D)})}{e} \quad (\text{eq. 12}),$$

$$[III] = \frac{([I_0] + [II_0]) f(D)}{e} \quad (\text{eq. 13}),$$

$$[F] = [I_0] + [II_0] - \frac{([I_0] + [II_0])(1 + f(D))}{e} \quad (\text{Eq. 14}),$$

where $f(D) = k_2 MD + k_1^2 MD^2 (2B+1)/4$, and I_0 and II_0 are the initial values for Form I and Form II respectively.

Croke and coworkers (1988) did not report the amount of fragmented DNA, but instead reported the amount of Form I, Form II, and Form III as a fraction of the total of Form I + Form II + Form III. For analysis of their data (see Discussion), the following formulas were used:

[I]

$$[I_f] = \frac{\text{_____}}{[I] + [II] + [III]} \quad (\text{eq. 15}),$$

[II]

$$[II_f] = \frac{\text{_____}}{[I] + [II] + [III]} \quad (\text{eq. 16}),$$

[III]

$$[III_f] = \frac{\text{_____}}{[I] + [II] + [III]} \quad (\text{eq. 17}),$$

where $[I_f]$, $[II_f]$, and $[III_f]$ are the fractional amounts of these species, and $[I]$, $[II]$, and $[III]$ are equations 11, 12, and 13, respectively.

DNAse I Digestions.

2 μ g of supercoiled pUC19 plasmid DNA was incubated with DNase I (final concentration 100 ng/ml) in 100 μ l buffer containing 50 mM Tris-HCl, 50 μ g/ml bovine serum albumin, and either 10 mM MgCl₂, or 0.66 mM MnCl₂. Incubations were carried out for various durations at 37°C, and were stopped by addition of 0.5 M EDTA to a final concentration of 20 mM EDTA. Following this incubation, 100 ng DNA from each time point was loaded on a 1% agarose gel, and electrophoresed at 100 volts (12.5 V/cm) for one hour. Gels were stained for 1.5 hours with ethidium bromide (0.4 μ g/ml), destained for 0.5 hours with dH₂O, and photographed as described above (see **Densitometry**).

RESULTS

Bipyrimidine Photoproducts were Reduced at High Intensity.

Irradiation of DNA with ultraviolet light (UV) causes the formation of cyclobutane dimers between adjacent pyrimidines. As UV dose increases, dimer levels do not continue to increase, but reach a plateau level (photosteady-state) that depends on the wavelength used. This plateau is a result of competing processes- the UV light not only induces the formation of the cyclobutane dimers, but also induces the dimer's reversal to the original pyrimidine monomers. At high doses the rate of dimer formation is balanced by the rate of dimer reversal, and a plateau dimer content is reached.

My experiments investigated whether the formation and photosteady-state plateau levels of pyrimidine dimers are not only wavelength dependent, but also intensity dependent. Figure 8 shows the effects of high and low intensity irradiation (high and low photon delivery rates, respectively) on the formation of T^T cyclobutane dimers. Following irradiation to indicated doses using either low (3.15×10^7 W/m²) or high (1.25×10^{11} W/m²) intensity UV light, tritiated DNA was acid hydrolysed to yield its constituent bases and

other products as described above (Materials and Methods). Dimer content was determined by two-dimensional paper chromatography. A plateau value was reached by about 10 kJ/m², at 4.2% and 2.8% of thymine residues in the DNA as T^T dimers for low and high intensity, respectively. The dose dependence of dimer formation was reduced at high intensity, as was the photosteady-state yield of dimers.

T^T dimers are the most abundant cyclobutane dimers formed (see DNA Photoproducts), but other pyrimidine dimers (T^C or C^C) also occur, albeit at lower levels. Figure 9 shows that formation of T^C dimers was also reduced at high intensity. Since the plateau levels are dependent upon the relative rates of dimer formation and dimer reversal, the lower plateau values of T^T and T^C seen at high intensity could be due to either a decrease in dimer formation or due to an increase in dimer reversal. I propose that the decrease in the photosteady-state level of dimers is due to a decreased rate of formation, as discussed below (see Discussion).

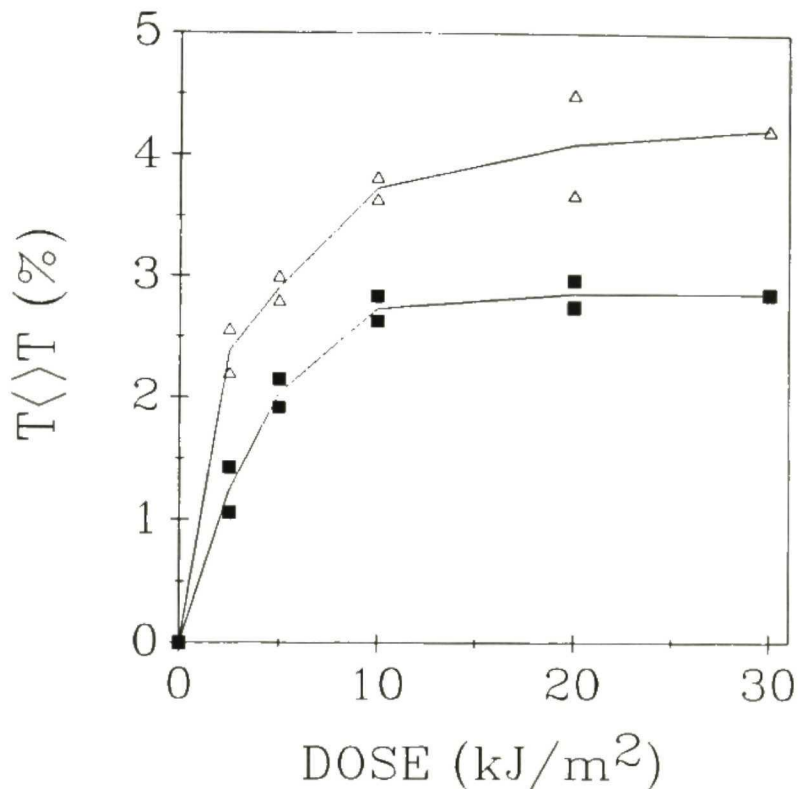


Figure 8- Formation of Thymine-thymine Cyclobutane Dimers (T<>T) in KrF Laser Irradiated DNA. Following irradiation of salmon sperm DNA labeled with [methyl-³H]thymine, samples were acid hydrolyzed and subjected to two-dimensional paper chromatography as described in **Materials and Methods**. Four independent experiments yielded results similar to those shown. Open triangles- $3.15 \times 10^7 \text{ W/m}^2$; solid squares- $1.25 \times 10^{11} \text{ W/m}^2$.

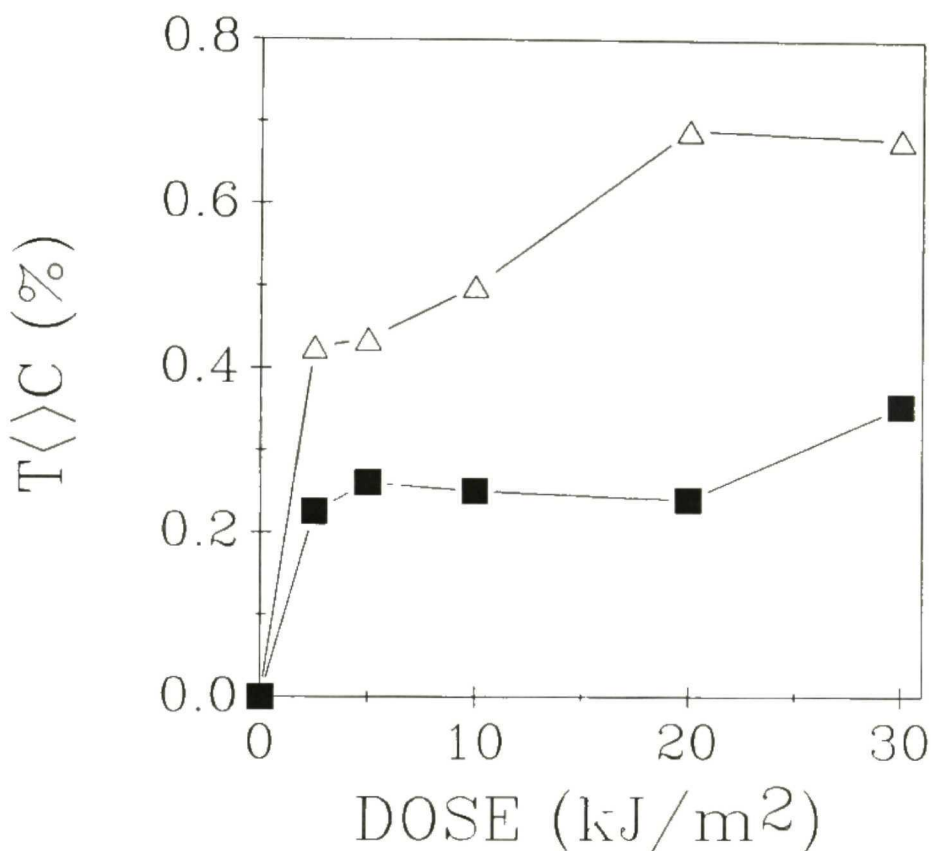


Figure 9- Formation of Thymine-cytosine Cyclobutane Dimers ($T<>C$) in KrF Laser Irradiated DNA. Following laser irradiation of salmon sperm DNA labeled with [*methyl-³H*]thymine, samples were acid hydrolyzed and subjected to paper chromatography as described in **Materials and Methods**. Four independent experiments yielded results similar to those shown. Open triangles- $3.15 \times 10^7 \text{ W/m}^2$; solid squares- $1.25 \times 10^{11} \text{ W/m}^2$.

Pyrimidine Photoadducts were also Reduced at High Intensity.

Cyclobutane dimers are the most abundant bipyrimidine photoproducts. Less numerous are pyrimidine photoadducts (see **DNA Photoproducts**), the most common of which is T(6-4)C. In contrast to cyclobutane dimers, bipyrimidine photoadducts are not reversed by UV light in the 240-280 nm range (Patrick and Rahn, 1976). Thus, the amount of T(6-4)C formed in DNA in my experiments (irradiation at 248 nm) should be linearly dependent on the dose- as the dose increased, all other things being equal, the number of T(6-4)C photoadducts made should have increased. Figure 10 shows the effect on T(6-4)C formation by irradiation at high and low intensity. It is apparent that the formation of T(6-4)C was linear with dose (in the evaluated dose range) for both high and low intensity, as expected. However, both the absolute amount of T(6-4)C made and the dose-dependence of its formation were decreased at high intensity, relative to low intensity irradiation. Since there was no competing back-reaction (photoreversal) at the wavelength employed, this decrease in the amount of T(6-4)C reflected a decrease in the formation of the dimer, and not an increase in its reversal.

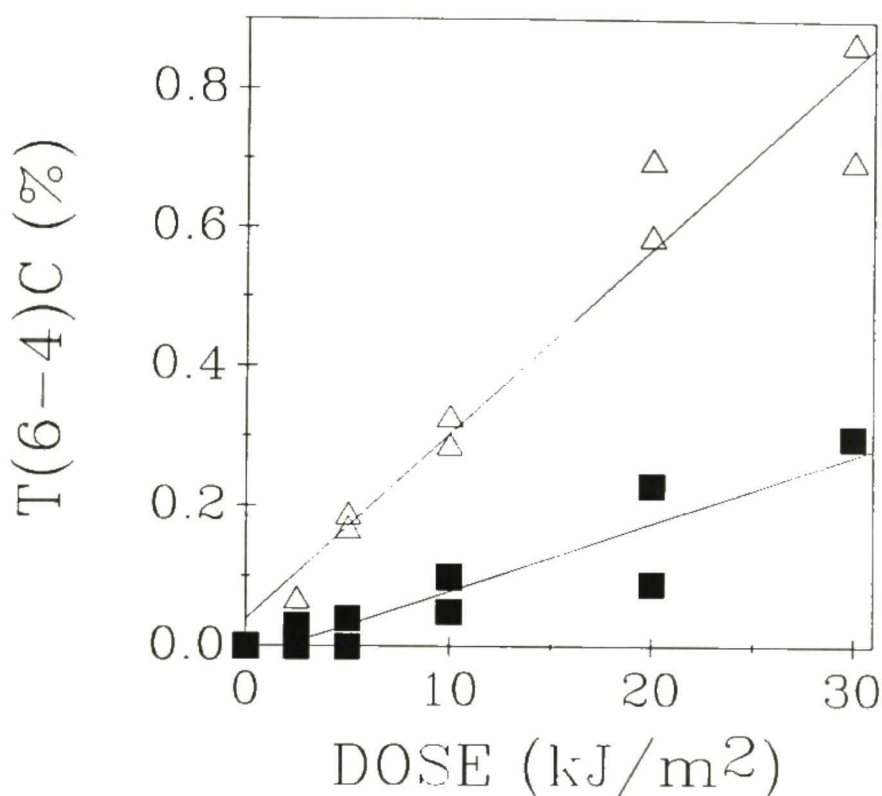


Figure 10- Formation of T(6-4)C in Laser Irradiated DNA. Following laser irradiation of salmon sperm DNA labeled with [*methyl-³H*]thymine, samples were acid hydrolyzed and subjected to two-dimensional paper chromatography as described in **Materials and Methods**. Four independent experiments yielded results similar to those shown. Open triangles- 3.15×10^7 W/m²; solid squares- 1.25×10^{11} W/m².

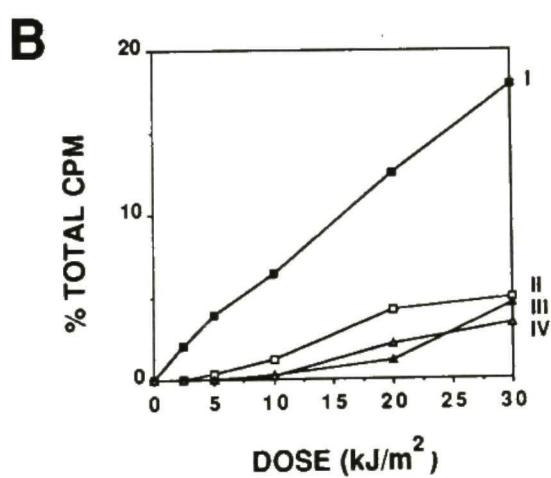
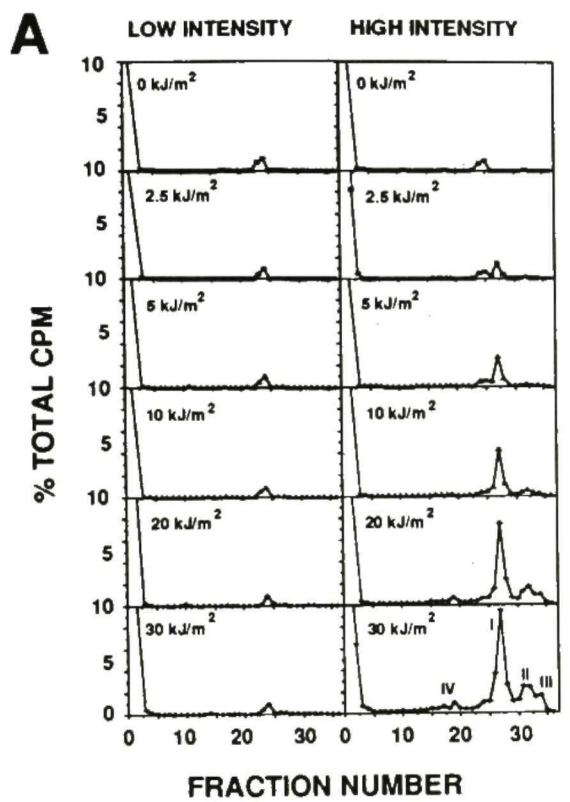
Thymine and Thymine Decomposition Products were Released from DNA Following Irradiation at High Intensity.

Following irradiation at high and low intensity, aqueous salmon sperm DNA radiolabelled with [*methyl-³H*]thymine was spotted on silica gel TLC plates and dried, the plates developed, fractionated, and analyzed as described in **Materials and Methods**. Figure 11A shows the results of this analysis. At low intensity, no release of any products from the phosphate backbone was noted. The peak at fractions 23-24 was present at all doses at the same level, and is a background peak of unknown nature. At high intensity, a dose-dependent release of low-molecular weight material from the DNA backbone was seen in the increasingly large peaks away from the origin. The largest peak, and the first to appear, corresponds to thymine by R_f . The other three peaks were not identified, but are assumed to be thymine degradation products, as thymine is the only labeled species in the DNA samples. Figure 11B shows the summation of the counts represented under each peak in Figure 11A, plotted against dose delivered at high intensity. From these two figures, the occurrence of ionizing events during irradiation at high intensity can be inferred (see **Discussion**).

Figure 11- TLC Separation of Thymine and Thymine Decomposition Products Released from DNA Following Laser Irradiation.

Panel A: salmon sperm DNA labeled with [*methyl-³H*]thymine was irradiated at low intensity (3.15×10^7 W/m²) or high intensity (1.25×10^{11} W/m²) to the final doses indicated, followed by TLC as described in Materials and Methods. The TLC lanes were each divided into 36 fractions and scintillation counted. Low intensity irradiation at all doses yielded no detectable release of thymine or thymine derived photoproducts. The nature of the background peak at fraction 24, which was present in all samples, is not known. Its mobility was less than that of free thymine, which was found at fraction 27. High intensity irradiation resulted in the release of at least four detectable products indicated in the lower right-hand box as I-IV. Peak I, which centered at fraction 27, co-migrated with authentic thymine marker. The other peaks have not been identified.

Panel B: the counts/min in the peaks identified in Figure 11A (I-IV) were summed and plotted as a function of dose delivered at high intensity. Peak I co-chromatographed with free thymine, whereas the other detectable products were not identified.



These DNA samples were labeled only in thymine; therefore, similar events in other residues could not be seen. However, there is no reason to suspect that a similar effect does not occur with the other bases. Indeed, investigations by others (Budowsky *et al.*, 1985; Croke *et al.*, 1988; Kovalsky *et al.*, 1990) suggest that the residue most susceptible to damage at high UV intensity is guanine. My results in this experiment are qualitatively similar to findings by others, where high intensity UV irradiation of DNA constituents led to degradation of the bases and scission of the glycosylic bond between base and sugar (studies with thymine, adenine, deoxyadenosine and uridyl-(3'-5')-uridine) (Menshonkova *et al.*, 1980; Budovskii *et al.*, 1981; Rubin *et al.*, 1981; Harrison, 1984). As seen in Figure 11B, a considerable number of DNA bases (up to approximately 25% of the thymine residues, and perhaps a similar number of other residues) were damaged or lost by high dose, high intensity UV irradiation, leaving fewer bases attached to the DNA and able to participate in normal photoproduct formation (see Discussion).

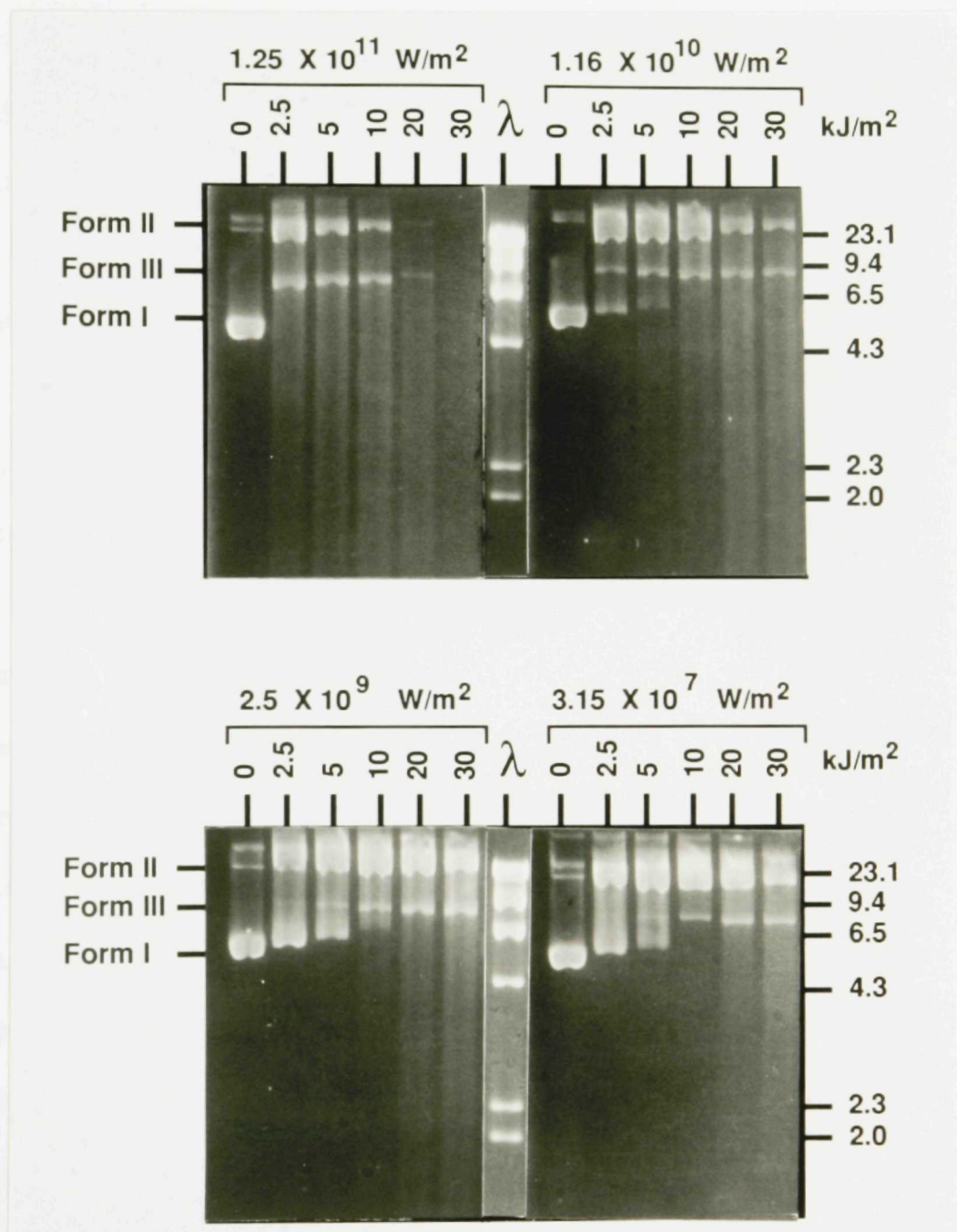
DNA Strand Breakage was Dose and Intensity Dependent.

Figure 12 shows electrophoresis of irradiated M13 RF DNA. Six different doses were used at each of four intensities. As the intensity increased at any one dose, the number of photons delivered to the sample remained the same, and the time over which the photons were delivered (total irradiation time) became increasingly short. The amount of damage sustained by the DNA was clearly dose dependent. As dose increased, Form I DNA decreased and Forms II and III DNA accumulated, regardless of the intensity employed. In addition, there was the appearance of a broad smear of DNA, which represents linear pieces of DNA that are less than unit length (termed here as "Form F"). As Form F DNA accumulated, the total amount of DNA in the Form I, II, and III bands diminished; eventually, with sufficient damage to DNA, these three forms disappeared entirely, and were replaced exclusively by Form F DNA, which (under electrophoresis conditions employed) sometimes ran off the gel, leaving the impression that no DNA was left in the lane. If one compares the same dose of UV light across the four intensities employed, one can see that increasing intensity caused increasing damage; the same number of photons delivered over a shorter period of time caused an increase in the damage

sustained by the DNA. This can be seen if one compares the amount of DNA in Forms I, II, and III at the four intensities at the 2500 J/m² dose point. There was clearly a greater shift from Form I to Forms II and III as intensity increased.

Figure 12. Gel Electrophoresis of Irradiated Samples.

Photograph of the ethidium bromide stained gels of M13 RF DNA samples irradiated in water to doses of 0-30 kJ/m², at each of four intensities (as indicated). Numbers on right side indicate size, in kilo-basepairs, of *Hind*III digestion fragments of λ DNA. Form I (supercoiled), Form II (open circular) and Form III (linear) DNA migrated as indicated. Form F DNA is considered to be that DNA in the smear extending towards the bottom of each lane. Increasing damage (strand breaks) to DNA is seen as accumulation of Forms II, III and F, with decrease in the amount of Form I, and is readily observed with increasing dose, and at the same dose with increasing intensity.



Conformational Changes Cannot be Attributed Solely to Single-Stranded Breaks.

The induction of nicks (single-stranded breaks; SSB) by high intensity UV has been previously reported (Budovskii et al., 1981; Gurzadyan et al., 1981; Nikogosyan et al., 1984; Schulte-Frohlinde et al., 1985; Opitz and Schulte-Frohlinde, 1987; Croke et al., 1988). An interesting feature of the gel seen in Figure 12 is that at several different experimental points, one can see that Forms I, II, and III coexisted in the same lane. The appearance of Form II following irradiation of Form I DNA was not surprising- a single nick in the DNA backbone is sufficient to convert a Form I supercoiled molecule to a Form II open circular molecule. The presence of linear Form III molecules was also not surprising at high doses and high intensities. As a Form II circle is progressively damaged by higher doses of UV, it will accumulate numerous SSB's. Eventually, two SSB's will occur on opposite strands sufficiently close together that the DNA can denature between the nicks, and create a linear molecule. However, it was surprising to find Form III molecules at the same time that one sees Form I molecules. In order for Form III to appear from Form II DNA, Form II must accumulate a large numbers of random SSB's, so that two such SSB's are

sufficiently close together to create a Form III molecule. For the lanes where one finds Forms I, II, and III coexisting, there must have been DNA molecules that have a large number of SSB's (to create a Form III plasmid from a Form I or Form II plasmid) at the same time that there were Form I molecules with no SSB's at all (as only one nick is required to transform Form I to Form II). Since care was taken to insure that all DNA molecules in a sample were evenly irradiated, one would expect that all molecules in a sample had a similar number of nicks, if one assumes a random distribution of such nicks.

The distribution of random discrete events (such as the nicking of DNA) can be described by a Poisson distribution (Armitage, 1971; Kroeber and LaForge, 1980). Such a distribution can be used to determine the probability of a DNA molecule sustaining "x" number of nicks, assuming an average of "m" nicks per molecule (Figure 13). If one assumes that there are two nicks per molecule on average ($m=2$, the minimum number of nicks one can have to create a linear molecule), one sees from the distribution that a significant number of molecules have either one or no nicks (approximately 25% each). Under these conditions, one would see supercoiled (no nicks) and circular (one nick) molecules coexisting with molecules having two nicks. With respect to the conformation

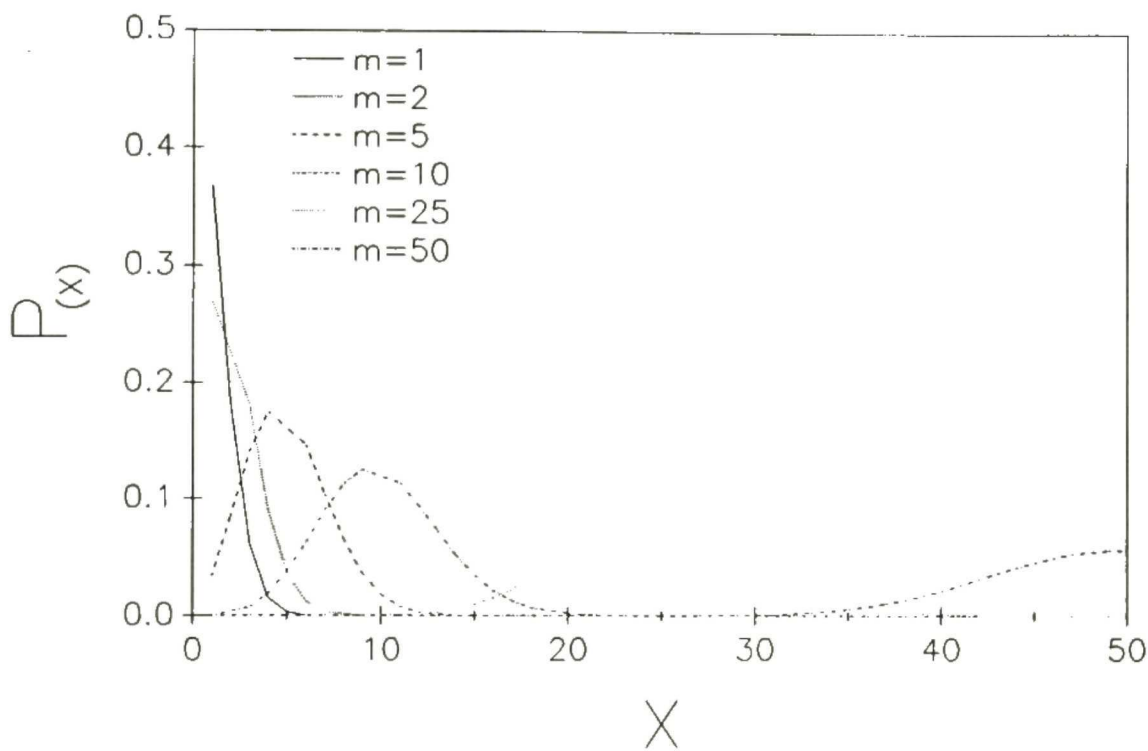


Figure 13- The Poisson Distribution. The Poisson distribution can be used to determine the probability of a DNA molecule sustaining "X" number of SSB's ($P_{(X)}$), assuming that an average DNA molecule has sustained "m" SSB's. Probabilities for X=0 to 50 SSB's are plotted for m=1, 2, 5, 10, 25 and 50 SSB's per molecule on average.

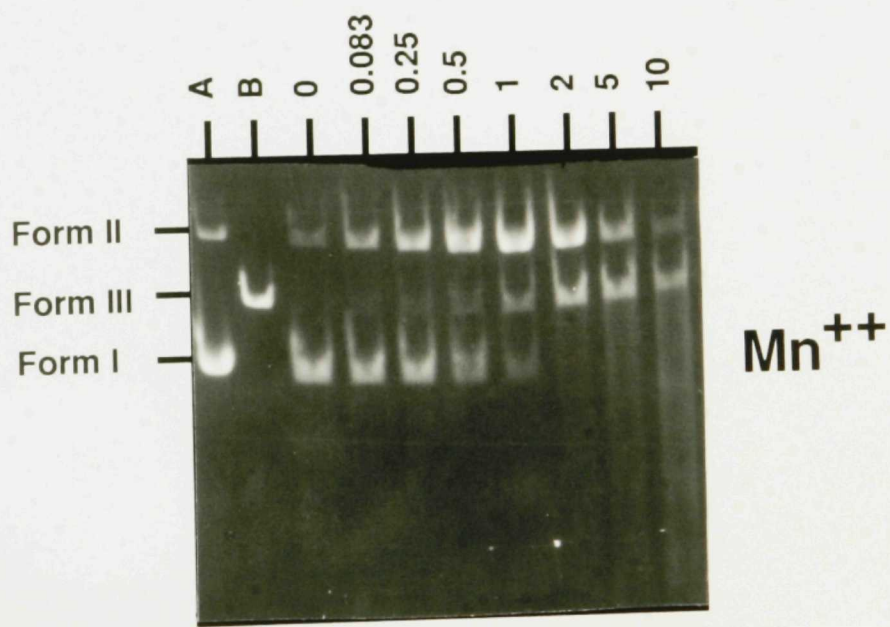
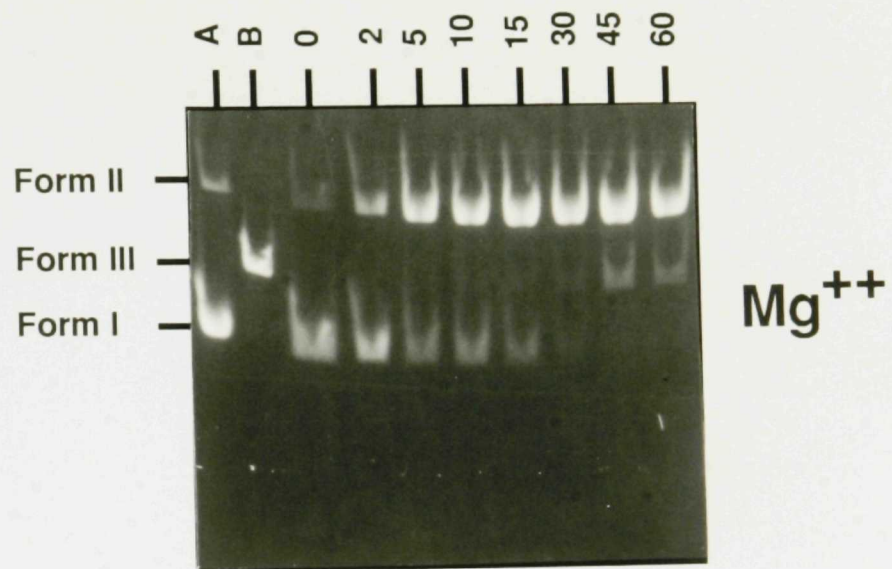
of molecules with two nicks, it is exceedingly unlikely that two nicks will be close enough together to create a double-stranded break. In pUC19, any such two nicks are likely to be many hundreds of base pairs apart; the distance would be even greater in the larger M13 RF DNA. Thus, a molecule with two random nicks would be circular rather than linear. If one assumes a greater average number of nicks, so that two may randomly fall close enough together to create a double-stranded break (requiring many nicks per molecule; $m=25$ or 50 in Figure 13), one sees that the probability of a molecule surviving unscathed is essentially zero. It follows that the simultaneous presence of Form I and Form III cannot be due to randomly located single-stranded breaks (nicks) alone.

A Defined Enzymatic System that Induced Single-strand Breaks (SSB's) and Double-strand Breaks (DSB's).

Figure 14 shows the results of digestion of pUC19 plasmid DNA with DNase I in either Mg^{++} or Mn^{++} containing buffers. In the presence of $MgCl_2$, it is known that DNase I creates random SSB's in DNA. In the presence of $MnCl_2$, DNase I creates DSB's as well as SSB's in DNA. Shorter times are used in the Mn^{++} buffer digestion because Mn^{++} , in addition to causing DNase I

to create DSB's, increases the rate of reaction of DNase I (Campbell and Jackson, 1980). Figure 14 shows that with SSB's only (Mg^{++} buffer), one sees the disappearance of Form I DNA, coupled to the appearance of Form II DNA. Form III DNA did not appear until essentially all the Form I DNA had disappeared, and the Form II DNA had accumulated sufficient SSB's such that two SSB's on opposite strands were sufficiently close to denature and form linear Form III DNA. On the other hand, in the presence of Mn^{++} , both DSB's and SSB's occur, resulting in the appearance of Form III DNA at times when Form I DNA was still present (0.25, 0.5, and 1 min points). This enzymatic system shows results that are similar to those seen in the 248 nm laser experimental system at high intensity- the coexistence of Forms I, II, and III. The results of the DNase I digestion in the presence of Mn^{++} suggest that laser irradiation produced DSB's or non-random opposition of SSB's in the plasmid DNA. This may be due to a single DSB inducing event or due to two SSB inducing events that are temporally and/or spatially coupled, occurring on opposite strands close to each other.

Figure 14. Gel Electrophoresis of DNase I Digests. Photographs of gel electrophoresis of supercoiled pUC19 DNA samples following digestion with DNase I in buffer containing either $MgCl_2$ or $MnCl_2$ as the divalent cation. Form I (supercoiled), Form II (open circular), and Form III (linear) DNA migrated as indicated. Lane A - a control that contained no enzyme. Lane B - pUC19 linearized by digestion with EcoR1. Other lanes are labeled with times of digestion as described below. The top gel shows results following digestion in Mg^{++} containing buffer; numbers at top show duration of digestion at $37^\circ C$ in minutes. The bottom gel shows results following digestion in Mn^{++} containing buffer; numbers at top show duration of digestion at $37^\circ C$ in minutes (0.083 minutes is five seconds).



Mathematical Modeling Demonstrated DSB's.

A mathematical model describing the effect of SSB's and DSB's on plasmid DNA conformation was developed (see **Materials and Methods**). The model used four equations to predict how much DNA will be in each of Forms I, II, III, and F given a starting amount of DNA in Forms I and II and a given dose of UV radiation. It contained two constants- **M**, the number of bases in the DNA (twice the number of base-pairs), and **B** (the overlap value), the maximum number of base-pairs by which two SSB's on opposite strands can be staggered without preventing intervening denaturation of the DNA and formation of a scission (an apparent DSB). The model can be fit for two parameters, k_1 and k_2 , the single and double strand break constants, respectively (k_1 is expressed in terms of SSB/base/J/m², k_2 is expressed in terms of DSB/base/J/m²). Calculations using hypothetical values for k_1 and k_2 were performed. When k_1 and k_2 both had positive, non-zero values, the resulting calculated curves describing how much DNA was in each form closely paralleled plotted experimental data. When k_1 was non-zero, but k_2 was set equal to zero (no DSB's occur), the calculated curves resembled the DNase I digestions with Mg⁺⁺, in that Forms I, II, and III could not coexist.

The modeling system I used (MLAB, from the Division of Computer Research and Technology at the National Institutes of Health) allows one to fit experimental data to the equations, and by using the least-squares method, will give the best fits possible by varying selected parameters. The equations were fit to my data by allowing k_1 and k_2 to vary with the constraint that $k_1 \geq 0$ and $k_2 \geq 0$ (negative values for k_1 and k_2 are meaningless), or by constraining $k_2=0$, and allowing only k_1 to vary. The former case allows for the occurrence of SSB's, DSB's, and apparent DSB's due to the close opposition of two independent SSB's. The latter represents the case that no DSB's occur, that only SSB's occur, and that all apparent DSB's are due to the opposition of two random, independent SSB's (i.e.- scissions). The results of these fits are shown in Figure 15. The left half of the figure (panels A, B, C, and D) shows results of model fits (various lines) to experimental points (plotted symbols) if k_1 and k_2 were allowed to vary (see figure legend). The right half of the figure (panels A', B', C', and D') shows results if the computer was allowed to fit only k_1 , and k_2 was constrained to zero. It is apparent that the values predicted by the model (plotted lines) more closely fit the actual experimental values (symbols) if both of the strand break constants were included. In addition, an objective measure of the goodness of fit, the

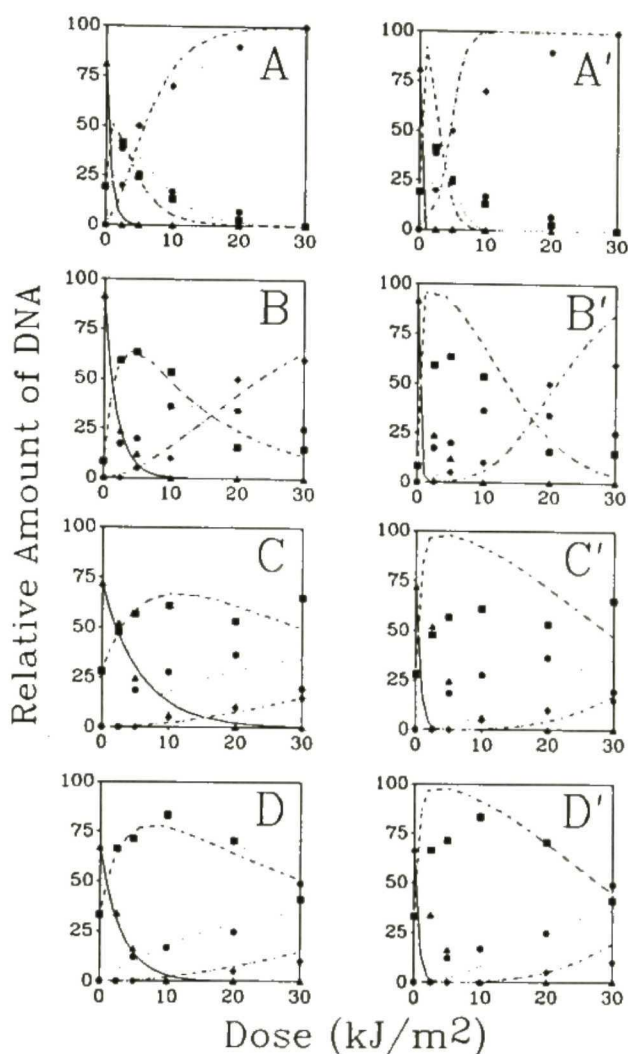


Figure 15. Results of Curve Fitting. Graphs show experimental data and fitted curves of experiments at four intensities: **A,A'**- $1.25 \times 10^{11} \text{ W/m}^2$; **B,B'**- $1.16 \times 10^{10} \text{ W/m}^2$; **C,C'**- $2.5 \times 10^9 \text{ W/m}^2$; **D,D'**- $3.15 \times 10^7 \text{ W/m}^2$. Symbols indicate experimental points: solid triangle- Form I (supercoiled) DNA; solid squares- Form II (open circular) DNA; solid circles- Form III (linear) DNA; solid diamonds- Form F (short linear) DNA. Lines indicate best fit curves for each form of DNA: solid line- Form I DNA; dashed line- Form II DNA; dotted line- Form III DNA; dashed-dotted line- Form F DNA. Left-hand panels (**A,B,C,D**) show results if curves were fit with non-zero values for both single and double strand-break constants. Right-hand panels (**A',B',C',D'**) show results if curves were fit with the double strand-break constant constrained to zero. See Results section for discussion.

sum of squares, was always smaller for the unconstrained fit than for the constrained fit, i.e. the sum of squares of the deviations of the model from the experimental points was smaller for the points with both k_1 and k_2 fit than with k_1 only. That is, if the model was constrained to $k_2=0$, it did much worse in describing what actually appeared experimentally than if one allowed k_2 to vary.

An additional measure of the goodness of fit is the **dependency value**, an arbitrary, dimensionless value from 0 to 1 that describes the dependency of one variable on another. To illustrate the nature of the dependency value, one can assume that one is using MLAB to fit the equation $ax^2+bx+c+d=y$ to a roughly parabolic set of data points. If one fits the equation to the data using only a , b , and c as variable parameters, one will get a reasonably close fit to the data, with a low sum of squares. However, if one uses all of the variable parameters in the equation (a , b , c , and d), one will find that, while a good fit with a low sum of squares is still possible, one will also get a high dependency value for c and d . This indicates that c and d are highly inter-related, as one can make significant changes to the value of one without altering the final shape, position, or quality of fit of the curve- one merely makes similar but opposite changes in the value of the other variable. Indeed, there is no difference

between $x^2+4x-5+6=y$ and $x^2+4x+100-99=y$. Two variable parameters with a low dependency value, on the other hand, are not related, and act as independent variable parameters. For example, there is a considerable difference between $5x^2+4x=y$ and $4x^2+5x=y$, and the dependency value for a and b is correspondingly small. A high dependency value, then, indicates that the equations being used do not accurately describe the data being fitted, as not all variable parameters that are fit to the data are independent of each other. If the dependency values for k_1 and k_2 were compared for fits where $k_2 \geq 0$ versus fits where $k_2=0$, it was seen that the dependency values for the unconstrained fits ($k_2 \geq 0$) were far better (smaller) than for the constrained fits (for example, the constrained fit may have had a dependency value $d=0.999$, while the unconstrained fit would have a dependency value $d=1 \times 10^{-4}$). In summary, the equations describing the effect of UV radiation on DNA conformation fit the experimental data best (with lowest sums of squares and lowest dependency values) when k_2 , the double-strand break constant, was greater than zero; the equations fit the data best when actual DSB's or non-randomly opposed SSB's were allowed to occur.

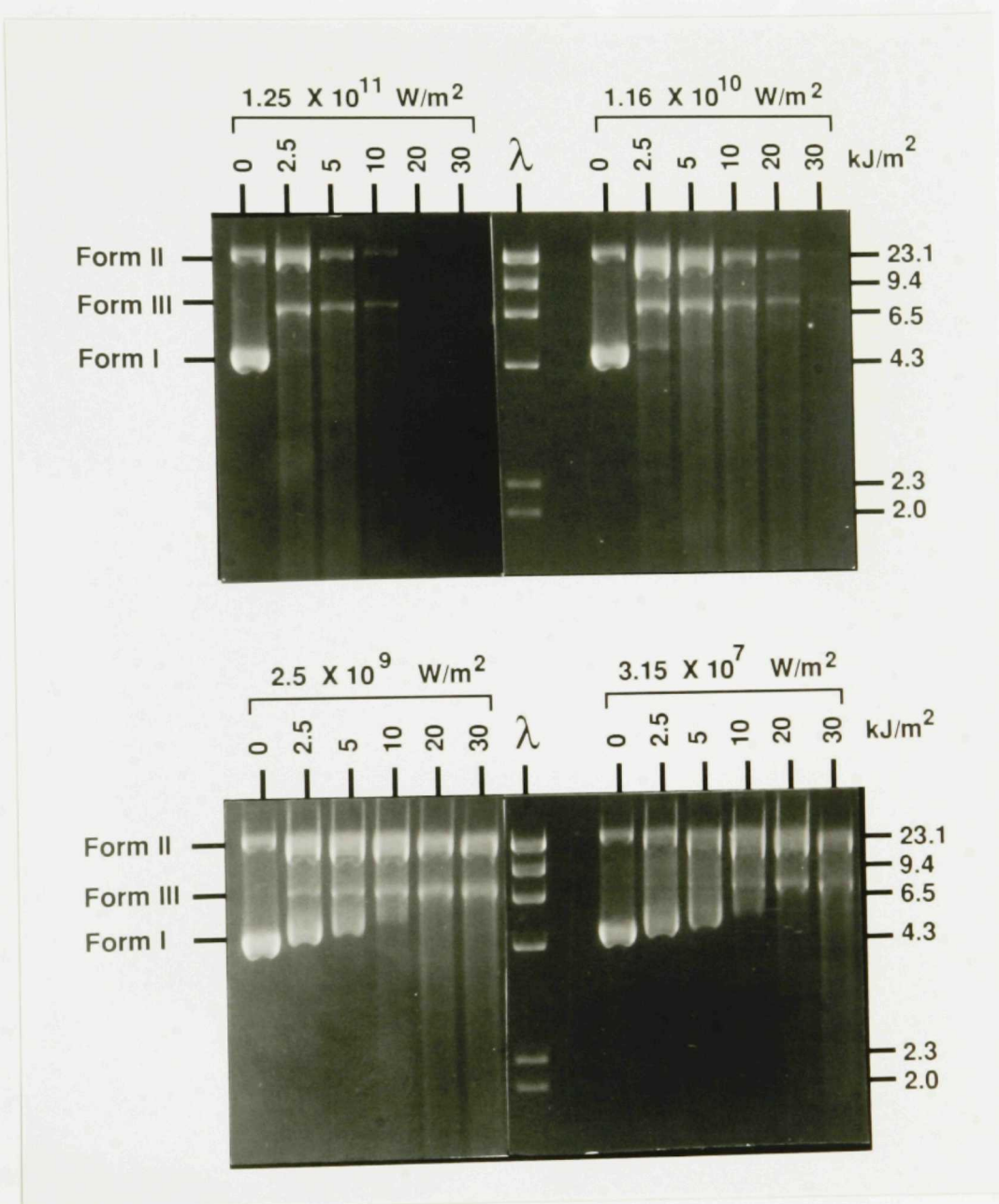
High Salt Concentration Did Not Alter Strand-break Damage to DNA.

To further test whether the apparent DSB's that were seen were indeed DSB type events or merely the close opposition of random SSB events, plasmid DNA was irradiated in 100 mM NaCl solution instead of in distilled water. Because high salt concentrations stabilize DNA (by diminishing electrostatic repulsion between phosphate groups in the backbone [Cantor and Schimmel, 1980]), one would expect to see less transformation of Form I to Form III DNA, if this transition was due to denaturation between random, closely spaced, opposed SSB's (von Sonntag *et al.*, 1981). This would give the appearance of less damage to the DNA following irradiation in 100 mM NaCl solution, as assayed by gel electrophoresis.

The result of such an irradiation in high salt solution is seen in Figure 16. This figure presents an experiment that was essentially identical to Figure 12, except that the DNA was irradiated in 100 mM NaCl solution instead of in distilled water. The resulting gel looks substantially similar to the gel in Figure 12; differences between the two gels were attributable to inter-experiment variation and, as shown below, were insignificant. Here again one sees apparent DSB's, as shown by the coexistence of Forms I, II, and III,

even under salt conditions anticipated to diminish the contribution to strand separation from random, closely spaced, opposed SSB's.

Figure 16. Gel Electrophoresis of Irradiated Samples.
Photograph of ethidium bromide stained gels of M13 RF DNA samples irradiated in 100 mM NaCl to doses of 0-30 kJ/m², at each of four intensities (as indicated). Numbers on right side indicate size, in kilobase pairs, of *Hind*III digestion fragments of λ DNA. Form I (supercoiled), Form II (open circular) and Form III (linear) DNA migrated as indicated. Form F DNA was considered to be that DNA in the smear extending towards the bottom of each lane (or having disappeared from the gel due to its small size). Increasing damage (strand breaks) to DNA was seen as accumulation of Forms II, III and F, with decrease in the amount of Form I, and was readily observed with increasing dose, and at the same dose with increasing intensity. The lane next to the λ DNA size marker lane was left empty.



Changing the Overlap Value (B) Did Not Eliminate DSB Events.

With respect to the analysis thus far discussed, it is still possible that all of the DSB events seen in my experiments were due to random SSB's on opposite strands. The equations take this possibility into account by including B , which should account for scissions occurring via random, opposite SSB's. Normally, k_1 and k_2 were fitted to experimental data using an overlap value of $B=10$ (Bothe et al., 1990). It is conceivable that under experimental conditions, two single-stranded breaks that were quite far apart could still cause the denaturation of DNA, and the appearance of DSB events. To test whether this occurred, the overlap value B was varied from $B=10$ to $B=500$. If there were no DSB events, the larger B value should include all denaturations from random single-stranded breaks. Figure 17 shows the results of fits for k_1 and k_2 as B was varied (this analysis used the same experimental data for all fits). In these fits, there was some decrease in the value of k_2 across all intensities as B increased, and a modest decrease in k_1 at the highest two intensities (10^{11} and 10^{10} W/m²). If all the apparent DSB's resulted from randomly apposed SSB's, one would expect k_2 to disappear as B was increased. Instead, one sees that at high intensity, k_2 had a non-zero value, even if B was

set at the high value of 500 (which means that two SSB's 500 bp apart could create an apparent DSB or scission). There was very little difference between the values determined for k_2 at reasonable values of B ($B=10$, 50, and even 100). This suggests that the apparent DSB's that were seen cannot be explained by the occurrence of random SSB's on opposite strands. Instead, there must be two coupled single-stranded breaks on opposite strands, either a true DSB, or two non-randomly opposed SSB's.

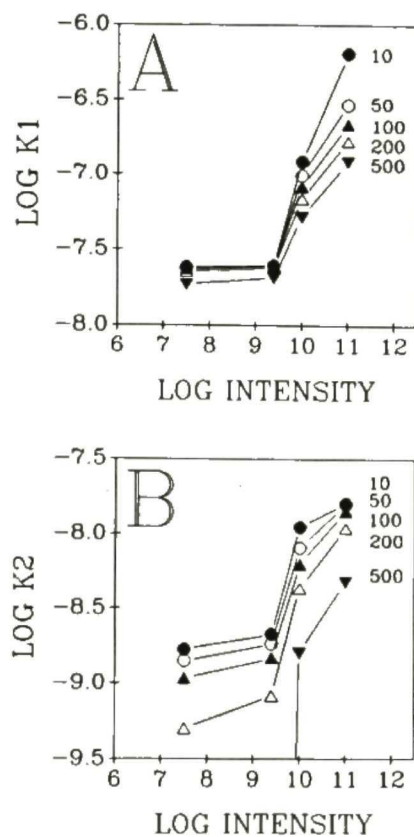


Figure 17. Effect on k_1 and k_2 of Varying Overlap Values (B).
Panel A: Graph showing effect of increasing overlap values on the single strand-break constant, k_1 . Identical data were fit to the model in all cases, the only difference was the overlap value used in each fit. Overlap values for each curve are indicated on the graph; solid circle, $B=10$; open circle, $B=50$; solid triangle, point up, $B=100$; open triangle, point up, $B=200$; solid triangle, point down, $B=500$.
Panel B: Graph showing effect of increasing overlap values on the double strand-break constant, k_2 . Symbols same as for panel A. See Results section for discussion.

Dependence of k_1 and k_2 on Intensity.

I found that k_1 and k_2 are constants only for a given intensity, and are altered at high intensities. Figure 18 shows the values of k_1 and k_2 determined by curve fitting to give the best fits of the model to experimental points. The top row of panels shows the value of k_1 versus intensity (panels A, B, and C), the bottom row shows the value of k_2 versus intensity (panels A', B', and C'). In panels A and A', M13 RF DNA was used, in panels B and B', pUC19 DNA was used. Panels C and C' show the average for all experiments, using both M13 RF and pUC19 DNA. The error bars are one standard deviation from the mean.

One can see from the graphs that as the intensity increased, the value of the strand-break constants, k_1 and k_2 , also increased, being higher at the highest intensity ($1.25 \times 10^{11} \text{ W/m}^2$) than at the lowest intensity ($3.15 \times 10^7 \text{ W/m}^2$). However, the increase was not linear. There was no significant change in the values for the break constants between the lowest two intensities ($3.15 \times 10^7 \text{ W/m}^2$ and $2.5 \times 10^9 \text{ W/m}^2$), while the value at the highest intensity ($1.25 \times 10^{11} \text{ W/m}^2$) was substantially higher. In both cases, the value for the break constants at about 10^{10} W/m^2 was intermediate between the lower intensities (10^7 and 10^9 W/m^2) and the

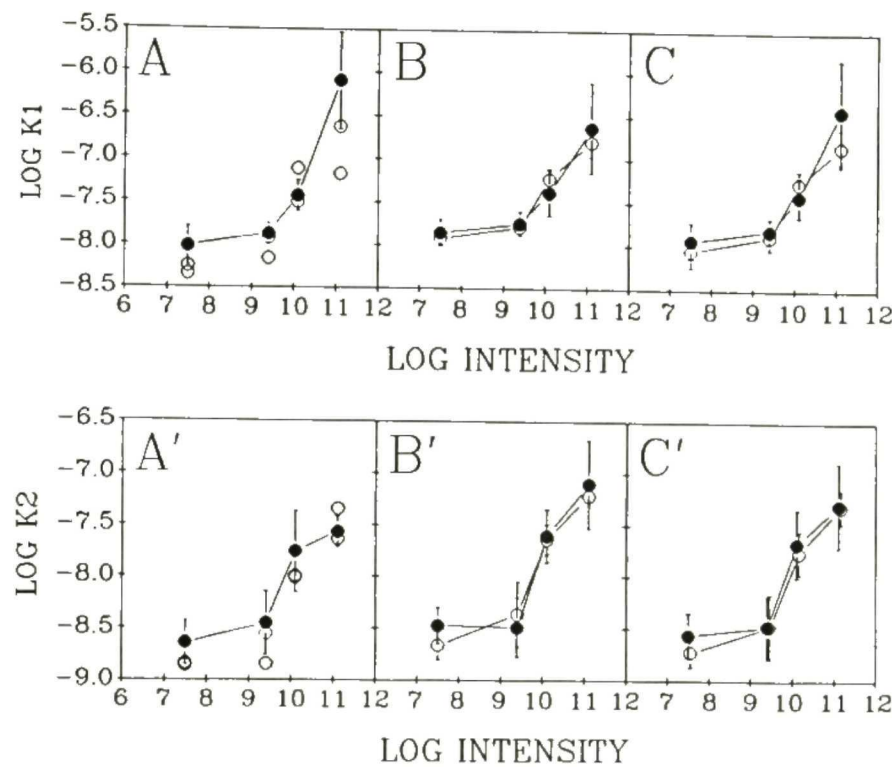


Figure 18. Values for k_1 and k_2 at Various Intensities. These graphs show the values of the logs of the single-strand break constant (k_1) and the double strand-break constant (k_2) at each intensity investigated. **A, A'** - average values for k_1 and k_2 , respectively, for experiments in which M13 RF DNA was used. Five irradiations in water (solid circle) and two in 100 mM NaCl (open circle) are plotted. **B, B'** - average values for k_1 and k_2 , respectively, for experiments in which pUC19 was used. Seven irradiations in water (solid circle) and five in 100 mM NaCl (open circle) are plotted. **C, C'** - average values for k_1 and k_2 , respectively, for both M13 and pUC19 experiments are plotted. Solid circles indicate irradiation in water, open circles indicate irradiation in 100 mM NaCl. In all graphs, the average value for Log k_1 or Log k_2 at each intensity is plotted; error bar shows one standard deviation from the mean. In panels **A** and **A'**, only two salt experiments were performed, and actual experimental values for log k_1 and log k_2 are plotted in that case.

highest intensity (10^{11} W/m 2). For k_1 , not only does the value increase with intensity, but the rate of change also increased with intensity, as shown on these log-log plots. There was a slight increase between 10^9 W/m 2 and 10^{10} W/m 2 , but a larger increase between 10^{10} W/m 2 and 10^{11} W/m 2 . For k_2 , there was little or no change between the lowest two intensities (10^7 and 10^9 W/m 2 , a difference of two orders of magnitude of intensity), and a significant increase between the middle two intensities (10^9 and 10^{10} W/m 2 , a difference of only one order of magnitude). There was an additional, though smaller increase between the highest two intensities (10^{10} and 10^{11} W/m 2).

This figure also shows what was noted in Figure 16- that high salt concentration makes no difference in the amount of strand-breakage that occurs following UV irradiation of DNA. The open circles indicate the values of k_1 and k_2 determined from experiments conducted using 100 mM NaCl solution instead of distilled water. It is apparent that there was no statistically significant difference between the values of k_1 and k_2 for irradiations carried out in distilled water and in high salt buffer. One also sees that, as in distilled water irradiations, there was a significant, non-linear increase (as seen in these log-log plots) in the values of k_1 and k_2 , as intensity increased.

The reason the increase was non-linear is because the events occurring were non-linear. At low intensities (10^7 and 10^9 W/m²), only one UV photon gets absorbed at any one target site in the DNA. However, as intensity increased from 10^9 to 10^{11} W/m², the photon density increased until there were enough photons at the target site that more than one photon could be absorbed. As would be expected, two photon processes typically show a 2° order dependence and are consequently non-linear with respect to intensity (Nikogosyan and Gurzadyan, 1984; Zavilgelsky et al., 1984; Opitz and Schulte-Frohlinde, 1987; Croke et al., 1988; Nikogosyan, 1990).

The energy deposited by two photons would be sufficient to cause base ionization. I have shown earlier that the absorption of the second photon causes the fragmentation of bases and formation of apyrimidinic sites (Figure 11A). It would also appear from the strand breakage data that ionized bases create breaks in the DNA backbone, mostly single stranded breaks (k_1 is several-fold higher than k_2), but also some apparent double-stranded breaks. The issue of whether true double-stranded breaks occur via a single bi-photonic event, or if there are two single-stranded breaks (requiring two bi-photonic events) that are non-randomly associated on opposite strands in close proximity has not yet been resolved, but does not change the validity of these results.

DISCUSSION

Investigators that have explored the effect on DNA and DNA components of high intensity ultraviolet radiation (see review by Nikogosyan, 1990) have found qualitative and quantitative differences in the amount and type of damage sustained by the DNA and its components following high intensity irradiation (10^{11} - 10^{12} W/m²), as compared to irradiation at low intensity (10^8 - 10^9 W/m² and lower). These differences in damage are attributable to the fact that at high intensity, multi-photon events occur where a DNA base absorbs a second photon within the excited state lifetime. Experiments show that below approximately 10^8 - 10^9 W/m², DNA-UV interactions are single quantum in nature; as the intensity increases, an increasing proportion of bi-photonic events occurs, until a saturation is reached where essentially all UV-DNA interactions are multi-quantum in nature. This saturation occurs between 10^{11} W/m² and 10^{13} W/m², depending on the investigator and experimental system (Rubin et al., 1981; Nikogosyan et al., 1982; Ballini et al., 1983; Angelov and Cadet, 1986; Croke et al., 1988; Masnyk et al., 1989). My early work investigated bipyrimidine photoproducts in DNA and showed a difference between high (10^{11} W/m²) and low (10^7 W/m²)

intensity irradiation, reflecting the one and multi-quantum events that are expected. Later work concentrated on damage to the DNA backbone.

Figure 4 illustrates the transitions from ground state to excited states and various routes of decay to stable endproducts. This schematic diagram can be applied to thymine, or other DNA constituents. With the absorption of a single UV photon ($h\nu_1$), thymine advances from the ground state S_0 to the lowest lying singlet excited state S_1 . Decay of S_1 to more stable states occurs via nonradiative thermal decay (internal conversion), fluorescence, intersystem crossing to the lowest triplet state T_1 , or through photoproduct formation. T_1 may decay to ground state by thermal processes (internal conversion), phosphorescence, or by covalent modification to form photoproducts. Absorption of a second photon, $h\nu_2$, by a thymine in S_1 or T_1 results in the promotion of the base to a higher excited state, S_1 to S_2 (or higher states), T_1 to T_2 (or higher states). In either case, the energy deposited exceeds the ionization constant for thymine. The triplet state of thymine in water has an energy estimated at 3.2 eV (Rubin et al., 1981); the energy of the singlet state is slightly higher. The addition of a second photon (248 nm, about 5.0 eV) leads to the deposition of a total of 8.2 eV, which is higher than the ionization level of

thymine (7.6 eV in water), and likely to lead to ionization of the base (Rubin et al., 1981). Thus, thymine may decay to stable, ground state products by fragmentation (following ionization), a manner qualitatively different from the decay of the less energetic states S_1 or T_1 .

Experiments by others have determined the lifetimes of singlet and triplet excited states of bases and nucleotides in aqueous solution. For the singlet state, S_1 has a lifetime on the order of 1-10 psec (Lamola, 1970; Daniels and Hauswirth, 1971; Hauswirth and Daniels, 1971a; Hauswirth and Daniels, 1971b; Lamola and Eisinger, 1971; Daniels, 1976; Oraevsky et al., 1981; Nikogosyan et al., 1982). The lifetime of the triplet state is much longer, on the order of microseconds at room temperature (Lamola and Eisinger, 1971; Whillans and Johns, 1971; Salet and Bensasson, 1975). The lifetimes of these states in DNA have not been accurately measured due to technical difficulties, especially with regards to measuring the lifetime of the triplet state. Such determination are usually made by exciting the DNA, then observing the resultant fluorescence (for singlet state excitation) or phosphorescence (for triplet state excitation) as the DNA decays to the ground state. Difficulties arise from the low level of DNA fluorescence and from the quenching of DNA phosphorescence in aqueous solution at room

temperature; at 25°C, most excited states relax through internal conversion, losing energy as heat. Such fluorescence and phosphorescence is easily detectable at 77°K in glasses composed of ethelene glycol and water mixtures, and for this reason most studies have been carried out under these conditions. The occurence of excited state multimers and complexes (excimers and exciplexes) along with the possibility for energy transfer along the DNA molecule further complicate attempts to measure excited state lifetimes, but some progress has been made.

Singlet state lifetimes of DNA at room temperature in aqueous solutions have recently been determined by detecting fluorescence in single-photon counting experiments. These experiments involve the detection of rare fluorescent emissions following excitation at room temperature; many thousands of such photon measurements are made, after which an average time of fluorescent emission following excitation can be determined, thereby indicating the excited state lifetimes. Ballini and co-workers (1983) measured the lifetime of the singlet excited states in calf thymus DNA and in poly[d(A-T)], and found most of the excited states decayed faster than the limit of resolution of their techniques (<100 ps), but a fraction (about 20%) decayed with a half-life of 3 ns. This latter fraction was attributed to excimer

fluorescence (excimers are excited-state dimers, in which the absorbed energy is shared by two closely adjacent species, such as two bases in DNA). Rigler and co-workers (1985) also studied poly[d(A-T)], and found that the majority of decay occurred within about 90 ps, but minor populations with half-lives of 870 ps (3% of detected signal) and 9 ns (1% of detected signal) also existed. In contrast, Georghiou and co-workers (1985) looking at calf thymus and *E. coli* DNA, found two decay components; the major peak had a half-life of 6-10 ps, but a minority (15%) decayed with a longer life-time of 40-65 ps. Decay populations with longer half-lives were not found, though this could possibly have been because they constituted too small a fraction to be detected. While the issue of the actual lifetime of the singlet excited state in DNA has not yet been solved, it is apparent that the lifetime is on the order of picoseconds for the majority of molecules, with a possible minor population, consisting of a few percent of excited molecules, that has a lifetime on the order of, at most, a few nanoseconds.

As mentioned above, measurement of the lifetimes of triplet excited states is difficult because of quenching of phosphorescence at room temperature. Studies of DNA and DNA constituents in glasses (of ethylene glycol and water) at 77°K have demonstrated triplet excited state half-lives in DNA on

the order of 0.3-2 seconds (Hauswirth and Daniels, 1976). Extrapolation of these results to room temperature is not straight-forward, but best estimates are that the lifetimes of triplet excited states of DNA at room temperature are on the order of several microseconds (Ballini et al., 1983).

The importance of these various states with regard to the formation of bipyrimidine photoproducts is not known. The high intensity employed in this body of work (about 10^{11} W/m²) is about two orders of magnitude too small to result in an appreciable number of thymines in S₁ absorbing a second photon, due to the brevity of the S₁ lifetime. This is based on: 1) the previously established values for the absorption cross-section of thymine for S₀ to S₁ and S₁ to S₂ (or higher) transitions (the absorption cross-section of ground state thymine is similar to that of S₁ or T₁ excited thymine) (Beavan et al., 1955; Nikogosyan et al., 1982); and 2) the assumption that the excited state lifetime of thymine residues in DNA is the same as the major fluorescence lifetime in aqueous DNA at room temperature (less than 100 ps). A certain portion of singlet states do apparently exist in excimers or other relatively long-lived complexes, and have lifetimes of several nanoseconds. Triplet states, on the other hand, have a lifetime significantly longer than the 20 ns pulse of the laser. Thus both long-lived singlet states (excimers) and

triplet states have a good chance of being promoted through biphotonic interactions. At high intensity ($1.25 \times 10^{11} \text{ W/m}^2$), most of the triplets would absorb two photons, and thus this state would be at or near saturation for two-quantum interactions. At low intensity ($3.15 \times 10^7 \text{ W/m}^2$), very few of the triplet states, and essentially none of the singlet states would be subject to excitation by more than one photon, and virtually all interactions would be expected to occur by conventional single-photon pathways. This agrees with data from other labs (Nikogosyan *et al.*, 1982; Zavilgelsky *et al.*, 1984). It is conceivable that the DNA is not being damaged directly, but is secondarily damaged by water-derived radicals that form by biphotonic absorption of water; this is a major mechanism of DNA damage following gamma-ray irradiation of DNA (Nikogosyan, 1990). However, water does not absorb UV significantly at the wavelengths employed, and the intensities achieved do not lead to the generation of water-derived radicals (Budovskii *et al.*, 1981; Rubin *et al.*, 1981; Nikogosyan *et al.*, 1982; Schulte-Frohlinde *et al.*, 1985; Croke *et al.*, 1988; Nikogosyan, 1990). Any DNA damage seen is therefore due to direct absorption of UV by DNA.

Figures 8 and 9 show that cyclobutane bipyrimidine photoproducts are reduced at high intensity relative to low intensity. This can be due to the fact that either more

dimers are destroyed, or fewer are made. I propose that this decrease is due to the fact that at high intensity, there are fewer dimers made, because there is a smaller number of bases populating the triplet state (or possibly singlet excimeric states) available to participate in dimer formation. This decrease is due to the absorption by long-lived excited states of DNA of a second photon, leading to the promotion of these precursor bases to higher excited states, with subsequent ionization. The resulting ionized base does not undergo modification to create a cyclobutane dimer, but instead undergoes fragmentation, or causes breakage of the glycosylic bond, leading to release of the base. With the base fragmented and/or removed, it cannot make a dimer, and dimer levels diminish accordingly. The excited state that most probably absorbs the second photon is the triplet state. However, if experiments by Ballini and coworkers (1983) and Rigler and coworkers (1985) demonstrating long-lived excimeric singlet states prove correct, it may be that such excimers are also involved in multi-photon excitation under our conditions (maximum intensity $1.25 \times 10^{11} \text{ W/m}^2$).

The fact that the triplet state is absorbing two photons and subsequently ionizing the excited base can be seen in results presented in Figure 11. Salmon sperm DNA was irradiated at high and low intensity, and then, without any

other treatment, spotted onto silica gel TLC plates. Free thymine and thymine decomposition products were seen on chromatography following irradiation at high intensity, indicating that the thymine was released from the DNA backbone by cleavage of the glycosylic bond. This cleavage follows the formation of thymine ions and/or ion-radicals after the absorption by thymine of two photons leading to deposition of sufficient energy to elevate that residue above its ionization constant (Schulte-Frohlinde et al., 1985; Angelov and Cadet, 1986; Opitz and Schulte-Frohlinde, 1986). Similar results are seen by other workers investigating biphotonic interactions (Menshonkova et al., 1980; Budovskii et al., 1981; Harrison, 1984). A considerable number of thymine residues are involved in this type of reaction (Figure 11B), strengthening my assertion that the reason the levels of dimers are lower following high intensity irradiation is because the excited state precursors to dimers are being depopulated by the absorption of a second photon. Thus, the triplet state must be a quantitatively important precursor to bipyrimidine photoproduct formation.

In an earlier study, Zavilgelsky and coworkers (1984) used a picosecond laser to investigate the effect of laser irradiation on DNA. Because these lasers have very short pulse lengths of great intensity (up to 10^{14} W/m²), they are

able to create biphotonic events that involve the S_1 as the absorbing intermediate state, and thus eliminate the singlet state contribution to single photon DNA photochemistry (via depopulation of S_1 by promotion to S_{11}). Zavilgelsky and coworkers found that pyrimidine dimer formation was diminished at the very high intensities characteristic of picosecond lasers (10^{12} - 10^{14} W/m 2), but not at lower intensities, similar to those used in my experiments (10^9 - 10^{11} W/m 2). This result was used to argue that pyrimidine dimers are formed exclusively through the singlet excited state. My studies used a nanosecond laser, which creates biphotonic reactions only via triplet states. In my experiments, dimer levels were lower following irradiation at high intensity than following irradiation at low intensity, indicating that the triplet state was involved in the generation of pyrimidine dimers. These results contradict Zavilgelsky's conclusions, though the presence of dimers (at reduced levels) following irradiation at high intensity in my experiments indicates that some (but not all) dimers do arise from singlet excited states. It is possible that the techniques used by Zavilgelsky were not sensitive enough to detect the contribution of triplet states to the formation of dimers. Zavilgelsky and coworkers (1984) determined dimer formation by measuring changes in absorption after laser irradiation and comparing these values to changes

in absorption following additional irradiation by a low-pressure mercury lamp at pH 12. This technique detects only fairly large changes in dimer levels; in any case, they did not measure dimer levels directly as I have done, and may have thus missed the importance of the triplet state.

Other evidence supports my view that triplet states are involved in pyrimidine dimer formation- Sutherland and Sutherland (1970) performed experiments using ethidium bromide and DNA that demonstrated the participation of both singlet and triplet states in the formation of pyrimidine dimers. When complexed with DNA, ethidium bromide is capable of sensitized fluorescence by emitting energy transferred to it from DNA via the singlet excited state, but not the triplet state. Thus, the intensity of sensitized fluorescence of ethidium bromide-DNA complexes is proportional to the extent of singlet excitation of the DNA. On the other hand, ethidium bromide quenches dimer formation by accepting energy transferred from both singlet and triplet excited states in DNA. Sutherland and Sutherland (1970) showed that the amount of dimer quenching was greater than that of sensitized fluorescence, demonstrating that dimers were formed from both singlet and triplet excited states.

Figure 10 shows that the bipyrimidine photoadduct T(6-4)C is also made at lower levels following irradiation at high

intensity than it is following irradiation at low intensity. This decrease in the formation of the adduct presumably occurs for the same reason that it does for pyrimidine dimers- depopulation of the lowest triplet excited state by promotion to higher states that decay by other pathways. It has never been previously reported that T(6-4)C can be made through the triplet state. The prevailing view has been that T(6-4)C adducts are made only through the singlet state, based on the failure of triplet quenchers to decrease levels of T(6-4)C formation in DNA, and of triplet sensitizers to induce the formation of T(6-4)C.

Triplet quenchers are effective at reducing photodimerization of some pyrimidine monomers in solution. Fisher and Johns (1976), for example, showed that the photodimerization of uracil is decreased by the triplet quencher Mn^{++} , but the dimerization of thymine is virtually unaffected. They suggest that steric hinderance from the 5-methyl group of thymine inhibits the activity of the triplet quencher. Such steric hinderance would be much greater in DNA than in pyrimidine monomers, and the absence of an effect by triplet quenchers on photoadduct formation in DNA is not a strong argument against the involvement of the triplet state in the formation of such adducts.

Triplet sensitizers are used to induce the triplet excited state in DNA or DNA constituents following irradiation at wavelengths that do not normally induce DNA excitation. An example of a triplet sensitizer is acetone, which can be excited by light at 310 nm. Light at this wavelength is not strongly absorbed by DNA. Following irradiation by 310 nm light, the excited S_1 acetone undergoes intersystem crossing to T_1 with nearly 100% efficiency (Rahn and Patrick, 1976). The triplet state acetone has an energy above that of the triplet state of all the DNA bases, and decays to ground state in part by transferring its energy to thymine (or another base), elevating that molecule to the first triplet state (Figure 19). Elevation to the singlet state is not possible because the S_1 state of DNA bases is more energetic than either the S_1 or T_1 of acetone. Transfer occurs down the energy gradient only, from the T_1 of acetone to the triplet state of a base. Triplet sensitization is also possible because the T_1 acetone has a lifetime of several microseconds, and thus has ample opportunity to interact with DNA in solution. Experiments which attempt to induce pyrimidine dimers in DNA by irradiating DNA in aqueous acetone solution (e.g., 20% acetone by volume) with light at 310 nm are very successful. A relatively large percent of the thymine bases form dimers, as there is no photoreversal of pyrimidine dimers

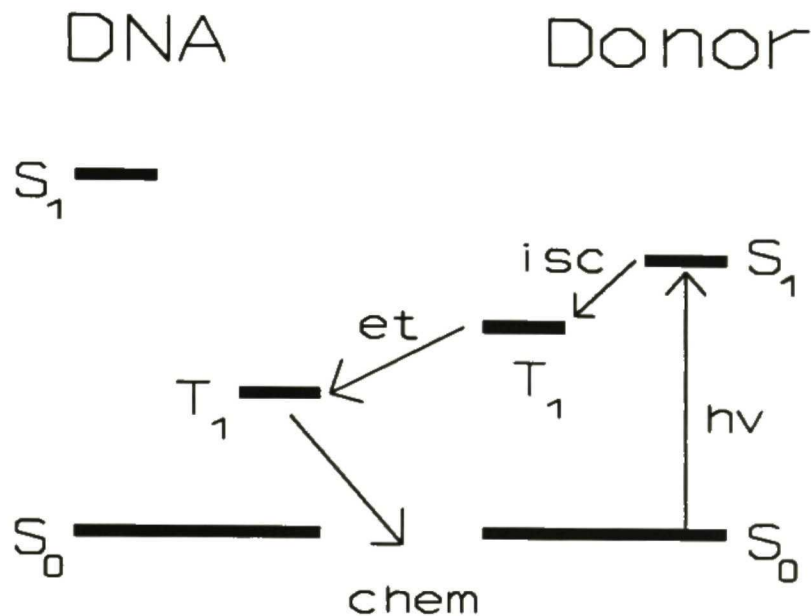


Figure 19- Triplet Sensitization. A triplet sensitizer (Donor) absorbs a photon ($h\nu$), and reaches the first singlet excited state (S_1); it undergoes intersystem crossing (isc) to the first triplet state (T_1). The energy is then donated (et-energy transfer) to DNA, promoting a base(s) to the triplet state (DNA), which decays to ground state (S_0), often by covalent modification (chem).

at 310 nm. However, attempts to use triplet sensitizers to make T(6-4)C photoadducts are generally unsuccessful (Wang, 1976a). This result has been used to argue that bipyrimidine photoadducts are made strictly through the singlet excited state. I have shown, however, that triplet sensitization conditions cause T(6-4)C photolysis (Masnyk et al., 1989). I, working with K. Minton and H. Nguyen, irradiated pre-formed T(6-4)C photoadducts in DNA in 20% acetone with light at 310 nm, and found that all the T(6-4)C adducts underwent photolysis, while the number of pyrimidine dimers, also present initially, increased. Therefore, the failure of triplet sensitizers to make T(6-4)C may be more due to its photolysis under the conditions employed for triplet sensitization than it is due to the fact that T(6-4)C is made only through the singlet state. Indeed, the fact that levels of T(6-4)C were decreased in my work following irradiation at high intensity argues that the triplet state (or possibly long-lived excimeric states) is involved in the formation of T(6-4)C, as high intensity irradiation at 10^{11} W/m² depletes the triplet state population available for adduct formation.

In addition to creating bipyrimidine photoproducts, UV irradiation of DNA under conventional conditions (low intensity, typically around 10 W/m²) is known to create single-stranded breaks in the DNA backbone, albeit rarely

(Rahn and Patrick, 1976; Nikogosyan, 1990). With sufficiently high doses, double-stranded breaks have also been seen following irradiation at low intensity (Moroson and Alexander, 1961). Part of this study concentrated on the effect of UV irradiation on DNA conformation and on the induction of strand breakage by UV light. As described above (see **Results**), strand breaks are also seen following irradiation at both low and high intensity in my work.

Several groups have conducted investigations evaluating strand breaks in DNA following irradiation at high intensity with UV light. Chilbert and coworkers (1988) used a xenon-chloride excimer laser (308 nm radiation) and *Bacillus subtilis* chromosomal DNA to specifically investigate strand-breakage in DNA. Schulte-Frohlinde and coworkers (1985) investigated strand breakage in poly-uridylic acid (poly-U). Zavilgelsky, Gurzadyan, and Nikogosyan (1984) investigated several forms of damage, among them strand-breaks, in poly-dT, using the fourth harmonic of a Nd:YAG laser. Croke and coworkers (1988) investigated strand-breaks in plasmid DNA using a KrF excimer laser. Gurzadyan and coworkers (1981) used a picosecond laser and supercoiled pBR322 DNA. Bothe and coworkers (1990) looked at calf thymus DNA following irradiation with a KrF excimer laser emitting UV light at 248

nm. Several other groups also performed similar experiments (Kovalsky et al., 1990; and Budowsky et al., 1985).

My results are generally consistent with all of these studies- all see two-photon events at high intensity, and all see an increase in the amount of strand-breakage, starting at about 10^{10} W/m². However, except for Bothe, no other group has detected DSB's. DSB events were not detected by other investigators for various reasons. Schulte-Frohlinde et al. (1985) and Zavilgelsky et al. (1984) used poly-U and poly-T, respectively, in their investigations; these are single-stranded polymers, precluding these investigators from seeing double-stranded breaks. Gurzadyan et al. (1981) used supercoiled pBR322 plasmid DNA and gel electrophoresis to follow conformational changes induced by strand breakage, but used relatively low doses (maximum dose 1800 J/m²), which may have prevented them from seeing double-stranded breaks. In addition, they did not use standard doses at varying intensities (as I have), making it more difficult to determine the effect of intensity on DNA conformation. Chilbert et al. (1988) used native DNA, but assayed strand breakage by alkaline sucrose gradient centrifugation. While this method is useful for determining the size of DNA fragments, it denatures DNA and thus allows observation of only single-stranded breaks.

Croke et al. (1988) on the other hand, independently used an experimental system that was very similar to mine, but interpreted their data in a qualitative fashion, in terms of single-strand breaks only. Croke used gel electrophoresis to assay strand breakage, and densitometrically scanned negatives of stained gel photographs to determine the amount of DNA in Forms I, II, and III. The range of intensities Croke and coworkers employed (10^9 to $5 \times 10^{12} \text{ W/m}^2$) was similar to the intensities I used (3.15×10^7 to $1.25 \times 10^{11} \text{ W/m}^2$). However, Croke and coworkers used much higher doses in their experiments than I did in mine. Whereas my experiments used standard doses of 0, 2.5, 5, 10, 20, and 30 kJ/m^2 for all intensities, Croke used doses of 2.5 kJ/m^2 to a maximum of approximately 340 kJ/m^2 , depending on intensity. Croke and coworkers found that as dose increases the amount of DNA in Forms II and III decreases. This is what I see as well- as dose increases, Forms II and III initially increase but then decrease in quantity. The question to ask is- where does the DNA go from Form III? If a Form III molecule is damaged by a sufficient number of SSB's or by one or more DSB's, it will fragment, and will migrate differently than either Form II or Form III. It becomes what I have called Form F (heterogeneous DNA of less than unit length). Croke and coworkers noticed that DNA disappeared with high dose, but did not

quantitatively account for fragmented DNA ("Form F"). These investigators' use of very high doses leads to the accumulation of extensive damage to the DNA. My experiments show that at high intensity, doses higher than approximately 10 kJ/m^2 lead to the accumulation of large amounts of DNA in Form F, with a rapidly decreasing percentage of the total DNA remaining in Forms I, II, and III.

Mathematical modeling demonstrated the existence of both single and double stranded breaks and allowed the calculation of SSB and DSB constants (k_1 , SSB/base/J/m²; and k_2 , DSB/base/J/m², respectively). Since Croke and coworkers presented large amounts of raw data, I attempted to discover if Croke and coworkers' data supported the occurrence of DSB's. Consequently, I fitted my model to their data. By digitizing data from their published figures, the relative amounts of DNA present in Forms I, II, and III were determined. After taking into account these values and the doses and intensities employed, I found that their observations are better explained if one does indeed assume the occurrence of DSB's. Because Croke and coworkers did not measure the total amount of DNA on the gel, I used a modified version of my equations- the equations were normalized to account for relative amounts of Forms I, II, and III. The normalization consisted of dividing the amount of DNA in any

one form by the total amount of DNA in all three measured forms (Forms I, II, and III), and was described in **Materials and Methods**. Figure 20 shows the results of my fits to Croke's data. The left-hand set of panels (panels A, B, and C) show fits if k_1 (the single-strand break constant) and k_2 (the double-strand break constant) are both fit to the data. The right-hand set of panels (panels A', B', and C') show fits if only k_1 is fit, and k_2 is constrained to $k_2=0$. It can clearly be seen that the model (plotted lines) better describes the experimental results (plotted symbols) if k_1 and k_2 are fit than if k_1 only is fit. Therefore, it appears that non-randomly opposed SSB's on opposite strands are occurring in the experiments of Croke et al. (1988) as well as in my experiments.

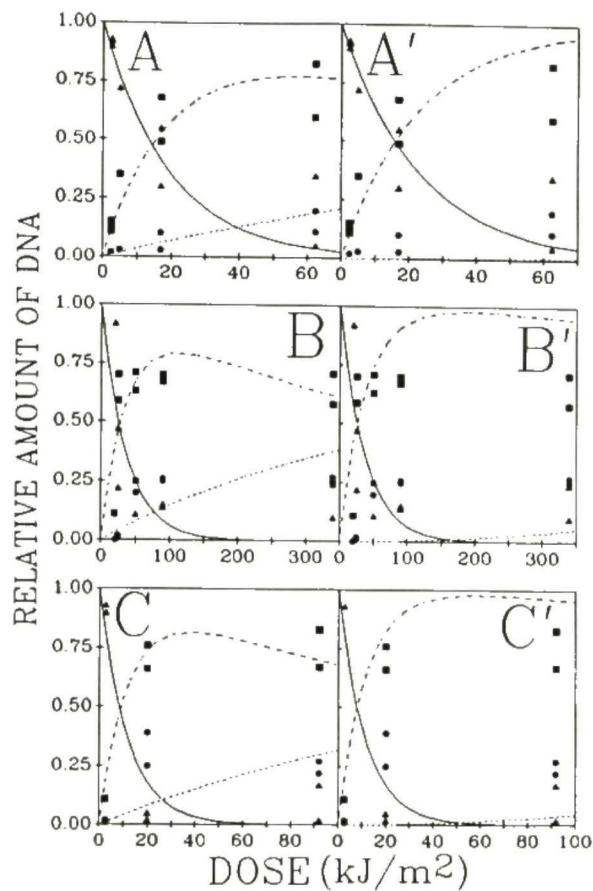


Figure 20. Results of Curve Fitting to Independent Data. Graphs show curves fitted to data derived from other investigators (Croke et al., 1988). Three intensities were used: **A,A'**- lowest intensity ($2.80 \times 10^{10} \text{ W/m}^2$); **B,B'**- middle intensity ($1.53 \times 10^{11} \text{ W/m}^2$); **C,C'**- highest intensity ($8.38 \times 10^{11} \text{ W/m}^2$). Symbols indicate experimental points: solid triangle- Form I (supercoiled) DNA; solid squares- Form II (open circular) DNA; solid circles- Form III (linear) DNA. Lines indicate best fit curves for each form of DNA: solid line- Form I DNA; dashed line- Form II DNA; dotted line- Form III DNA. Left-hand panels (**A,B,C**) show results if curves were fit with non-zero values for both single and double strand-break constants. Right-hand panels (**A',B',C'**) show results if curves were fit with the double strand-break constant constrained to zero. See Discussion section for details.

Figure 18 shows strand break-dose constants obtained at various intensities from my own data. In keeping with the two-quantum nature of DNA-UV photon interactions under consideration, one would expect to see little variation in the strand-break constant relative to intensity, until a certain threshold intensity was reached. One would then expect a rapid increase in the strand-break constant, consistent with second order intensity dependence with respect to triplet states. This is essentially what is seen. There is little variation in the strand break constants at the low intensities (10^7 and 10^9 W/m²), followed by a rapid increase in k_1 and k_2 values at the higher intensities (10^{10} and 10^{11} W/m²). This increase represents the transition between nearly exclusive single-photon UV-DNA interactions of singlet and triplet states (at 10^9 W/m² and below) and nearly exclusive two-photon UV-DNA interactions of triplet states (at 10^{11} W/m² and above) (Nikogosyan and Gurzadyan, 1984; Zavilgelsky, 1984; Opitz and Schulte-Frohlinde, 1987; Croke et al., 1988; Nikogosyan, 1990). At these higher intensities, singlet excited states remain unaffected by two-photon processes, unless S_1 undergoes intersystem crossing (isc) to the triplet state. The KrF excimer laser used, which emits 20 ns pulses of laser light, is unable to produce the higher intensities needed to achieve two-photon events via the singlet manifold (S_1 to S_2). This

occurs at intensities above 10^{12} W/m², and requires the use of a laser capable of emitting light of these high intensities, typically in a pulse only a few picoseconds long; in contrast, a KrF excimer laser is not able to deliver enough photons within its nanosecond pulse to achieve such intensities (Ballini, 1983; Angelov and Cadet, 1986).

Figures 17 and 18 also show that at high intensity (1.25×10^{11} W/m²) the value of k_1 is about thirty times that of k_2 (a difference of approximately 1.5 logs). This means that for every thirty SSB's, one should expect a DSB to occur, either directly or through two non-randomly opposed SSB's. However, at low intensity (3.15×10^7 W/m²), the difference between k_1 and k_2 is only about one log, or even less. This means that k_1 is only about five or ten times larger than k_2 . One might then expect a significant number of DSB's would occur at low intensity as well as at high intensity, despite the fact that experimentally, DSB's are seen at low intensity only at very high doses (Moroson and Alexander, 1961). One obvious explanation for this phenomenon is that the quantum yield for SSB's and DSB's at low intensity (as reflected by the low values of k_1 and k_2) are so low that they are at the limit of detection at conventionally employed doses. Even at high doses at low intensity, only SSB's will be detected,

explaining the requirement for very high doses at conventional intensities to observe DSB's (Moroson and Alexander, 1961).

The mathematical model used to calculate k_1 and k_2 contained several terms that affect the value of those constants: **M**, the number of bases in a DNA molecule; **D**, the dose of UV delivered; and **B**, the overlap value, or the minimum number of nucleotides separating two SSB's on opposite strands without the occurrence of a DSB or scission. The value of **M** and **D** are set by the experimental conditions. **M** varied depending on whether pUC19 or M13 RF DNA was used; in either case **M** was a well defined number. The dose that was delivered to each sample, **D**, was also well defined by the irradiation conditions. The value of **B**, on the other hand, was much less reliable. In most of the calculations, a value of **B**=10 was used, as this agreed with previously published results (Bothe et al., 1990). However, it is possible that the actual value of **B** is greater, as base modification occurs in parallel with strand cleavage (dimer formation and base ionization, Figures 8, 9, 10, and 11). Should such base modification occur between two SSB's on opposite strands of DNA, the extent of base pairing between the SSB's would be decreased, and the DNA might denature, creating a scission (Zavilgelsky et al., 1984). This would effectively increase the value of **B** to some value **B**>10. Indeed, Bothe and coworkers irradiated calf

thymus DNA with a KrF laser at 248 nm, and determined the yields of SSB's and DSB's. From these results, they calculated an overlap value of $B=40-70$, somewhat higher than my estimates of $B=10$ (Bothe et al., 1990). However, increasing the value of B from $B=10$ to $B=50$ does not alter my conclusion that double-stranded breaks or non-randomly opposed single-stranded breaks occur following irradiation of DNA at high intensity (see Figure 17 and corresponding text in Results).

Several investigators have attempted to determine the site of damage to DNA following UV irradiation at high intensity by using sequencing gels to look for specific cleavage patterns (Budowsky et al., 1985; Croke et al., 1988; Kovalsky et al., 1990). These investigators found that damage occurs predominantly not at thymine residues, but rather at guanine residues. This is due to the fact that guanine has the lowest ionization energy of the four bases, and possibly due to the migration of energy from nearby bases to guanine residues (Opitz and Schulte-Frohlinde, 1987; Croke et al., 1988; Kovalsky et al., 1990). Such an energy transfer could act to preferentially damage guanines by creating an energy sink. The excited state migrates across a few bases, then stops at guanine, which ionizes, precluding the further transfer of energy.

In contrast, I saw considerable damage in thymine residues. Thymine is readily damaged following UV irradiation at conventional intensities (indeed, T^T dimers predominate over other dimers), and one would expect continued damage to thymine following high intensity irradiation, as is indeed the case (Figure 11). However, since only thymine residues were labeled in my experiments, I would not have detected the release of free guanine or guanine fragments from the DNA backbone following irradiation. While it has been suggested that the release of bases by cleavage of the glycosylic bond following biphotonic reactions is confined in DNA to guanine residues (Kovalsky, personal communications), it is apparent from my experiments and those of Kovalsky and others (Budowsky et al., 1985; Croke et al., 1988; Kovalsky et al., 1990) that both thymine and guanine are affected by high intensity UV radiation. Both residues can absorb two photons, causing promotion of these bases to high lying excited states with subsequent ionization, bond cleavage, and release of free base. As discussed above, the excited state involved is probably the triplet excited state.

In my experiments, I saw both single-stranded and apparent double-stranded breaks in DNA irradiated at high intensity. However, my work cannot determine whether the DSB's that are seen are due to the non-random opposition of

two SSB's near each other (requiring two related biphotonic events), or due to true DSB events (requiring one biphotonic event). With regard to the latter speculation, Budowsky and coworkers (1985) have reported preferential base modification opposite previously altered bases, either within the same or in adjacent base pairs, suggesting a mechanism for the introduction of biased single-stranded breaks in opposition. Croke and others have shown that strand breaks occur preferentially near guanines (Opitz and Schulte-Frohlinde, 1987; Croke et al., 1988; Kovalsky et al., 1990), and it is therefore possible that double-strand breaks are favored at G-C base pairs. A means of introducing biased single-strand breaks in opposition to each other was suggested by Bothe et al. (1990), who proposed that DSB's may be in part due to radical transfer from the end of a cleaved strand to the complementary strand. Further research needs to be done to determine whether observed DSB's are due to one biphotonic event or two biphotonic events.

My experiments show the importance of long-lived excited states (triplet and possibly excimeric singlet states) in the generation of DNA damage by both single and multiple photon processes. Under conditions of nanosecond pulse high intensity laser irradiation (20 ns, 10^{10} - 10^{11} W/m²), long-lived excited states, but not short lived singlet states, are

promoted to higher level excited states by the absorption of a second photon; the higher level states decay to the ground state by means that differ both quantitatively and qualitatively from single photon excitation. The energy deposited in the base by two photons exceeds the ionization potential for a base. This in turn leads to the fragmentation of bases with formation of ions and ion-radicals with concomitant covalent bond cleavage: 1) of the phosphate backbone, leading to strand breakage; 2) of the glycosylic bond, leading to base release; 3) within the base itself, resulting in base derived ion-radical fragments, leading to base destruction, strand breakage, or glycosylic bond cleavage. Thus damage following two-photon excitation resembles to some extent damage induced in DNA by ionizing radiation (see **DNA Photoproducts**).

The depletion of long-lived excited states by promotion to high lying excited states means that few bases are available as the lowest triplet excited state or excimeric singlet excited state precursors for the formation of the more common forms of damage, found under low intensity irradiation conditions. Thus fewer bimolecular pyrimidine photoproducts are made following irradiation at high intensity than following irradiation at low intensity.

I have also shown the existence of an apparent double-stranded break in DNA irradiated at the intensities attainable with a KrF excimer laser. This DSB event may or may not be a true double stranded break; it may be due to two single-stranded breaks that are spatially and temporally associated, and occur on opposite strands. These DSB events could occur at an appreciable frequency following irradiation of DNA at intensities sufficient to cause two-photon DNA interactions. Such double-stranded breaks were previously seen only following irradiation of DNA with ionizing radiation.

The long-lived excited states that I have demonstrated may also be responsible for the generation of certain rare forms of damage that are not easily explained by conventional mechanisms. The minus-one frameshift mutations that occur in DNA following irradiation with UV-light at conventional intensities (10 W/m^2) are difficult to explain, but a recent proposal that they are caused by the formation of cyclobutane dimers between nonadjacent pyrimidines in the same strand requires that a DNA base exist in an excited state for a relatively long time, such that nonadjacent DNA bases may encounter each other (Nguyen and Minton, 1988). This notion is supported by my work. Finally, my experiments point out that the wavelength and dose of radiation are not the only determinants of DNA damage; the intensity used to irradiate

DNA is of equal importance in resolving the type and amount of damage sustained by the irradiated DNA.

BIBLIOGRAPHY

Angelov, D.A., and Cadet, J. (1986) "Recent aspects of the high power laser photophysics and photochemistry of nucleic acids and related components", in *Molecular Electronics* (Borisov, M., ed) pp 704-718, World Scientific Publishing, Singapore

Armitage, P. (1971) *Statistical Methods in Medical Research*, pp 66-72, Blackwell Scientific Publishers, Oxford

Ausbel, F.M., Brent, R., Kingston, R.E., Moore, D.D., Seidman, J.G., Smith, J.A., and Struhl, K., editors, (1989) *Current Protocols in Molecular Biology*, J. Wiley and Sons, New York

Ballini, J.P., Vigny, P., and Daniels, M. (1983) "Synchrotron Excitation of DNA Flourescence, Decay Evidence for Excimer Emission at Room Temperature", *Biophys. Chem.* 18:61-65

Beavan, G., Holiday, E., and Johnson, E. (1955) "Optical Properties of Nucleic Acids and Their Components", in *The Nucleic Acids* (Chargoff, E., and Davidson, J., eds) Vol. 1, pp 493-553, Academic Press, New York

Bothe, E.H., Görner, H., Opitz, J., Schulte-Frohlinde, D., Siddiqi, A., and Wala, M. (1990) "Single- and double-strand break formation in double-stranded DNA upon nanosecond laser-induced photoionization", *Photochem. Photobiol.* 52:949-959

Brau, Ch.A. (1984) "Rare Gas Halogen Excimers", in *Excimer Lasers* (Rhodes, Ch.K., ed) pp 87-137, Springer-Verlag, Berlin

Budowsky, E.I., Kovalsky, O.I., Yakovlev, D. Yu., Simukova, N.A., and Rubin, L.B. (1985) "Footprinting of DNA secondary structure by high intensity (laser) ultraviolet irradiation", *FEBS Lett.* 188:155-158

Budovskii, E., Simukova, N., Tikhonova, A., Menshonkova, T., and Rubin, L. (1981) "Two-photon photochemistry of nucleic acid components", *Sov. J. Quantum Electronics* 11:1602-1606

Campbell, V.W., and Jackson, D.A. (1980) "The effect of divalent cation on the mode of action of DNase I: the initial reaction products produced from covalently closed circular DNA", *J. Biol. Chem.* 255:3726-3735

Cantor, C.R., and Schimmel, P.R. (1980) *Biophysical Chemistry, Part III: The Behavior of Biological Macromolecules*, pp 1109-1181, W.H. Freeman and Company, San Francisco

Cerutti, P.A. (1976) "Base Damage Induced by Ionizing Radiation", in *Photochemistry and Photobiology of the Nucleic Acids* (Wang, S., ed) Vol 2, pp 375-401, Academic Press, New York

Chilbert, M.A., Peak, M.J., Peak, J.G., Pellin, M.J., Gruen, D.M., and Williams, G.A. (1988) "Effects of intensity and fluence upon DNA single-strand breaks induced by excimer laser radiation", *Photochem. Photobiol.* 47:523-525

Croke, D.T., Blau, W., OhUigin, C., Kelly, J.M., and McConell, D.J. (1988) "Photolysis of phosphodiester bonds in plasmid DNA by high intensity UV laser irradiation", *Photochem. Photobiol.* 47:527-536

Daniels, M., and Hauswirth, W. (1971) "Flourescence of the Purine and Pyrimidine Bases of the Nucleic Acids in Neutral Aqueous Solution at 300°K", *Science* 171:675-677

Daniels, M. (1976) "Excited States of the Nucleic Acids: Bases, Mononucleosides, and Mononucleotides", in *Photochemistry and Photobiology of the Nucleic Acids* (Wang, S., ed) Vol. 1, pp 23-108, Academic Press, New York

Fisher, G.J., and Johns, H.E. (1970) "Ultraviolet Photochemistry of Thymine in Aqueous Solution", *Photochem. Photobiol.* 11:429-444

Fisher, G., and Johns, H. (1976) "Pyrimidine Photodimers", in *Photochemistry and Photobiology of the Nucleic Acids* (Wang, S., ed) Vol. 1, pp 225-294, Academic Press, New York

Franklin, W.A., Lo, K.M., and Haseltine, W.A. (1982) "Alkaline Lability of Flourescent Photoproducts Produced in Ultraviolet Light-Irradiated DNA", *J. Biol. Chem.* 257:13535-13543

Georghiou, S., Nordlund, T., and Saim, A. (1985) "Picosecond Flourescence Decay Time Measurements of Nucleic Acids at Room Temperature in Aqueous Solution", *Photochem. Photobiol.* 41:209-212

Gurzadyan, G.G., Nikogosyan, D.N., Kryukov, P.G., Letokhov, V.S., Balukhanov, T.S., Belogurov, A.A., and Zavilgelsky, G.B. (1981) "Mechanism of high power picosecond laser UV inactivation of viruses and bacterial plasmids", *Photochem. Photobiol.* **33**:835-838

Häder, D., and Tevini, M. (1987) *General Photobiology*, pp 65-89, Pergamon Press, Oxford

Harrison, C.A., (1984) *Photochemistry of Nucleic Acids Including Crosslinking to Proteins*. PhD thesis, University of Rochester

Hauswirth, W., and Daniels, M. (1971a) "Radiationless Transition Rates of Thymine and Uracil in Neutral Aqueous Solution at 300°K", *Chem. Phys. Lett.* **10**:140-142

Hauswirth, W., and Daniels, M. (1971b) "Flourescence of Thymine in Aqueous Solution at 300°K", *Photochem. Photobiol.* **13**:157-163

Hauswirth, W., and Daniels, M. (1976) "Excited States of the Nucleic Acids: Polymeric Forms", in *Photochemistry and Photobiology of the Nucleic Acids* (Wang, S., ed) Vol. 1, pp 109-167, Academic Press, New York

Kovalsky, O.I., Panyutin, I.G., and Budowsky, E.I. (1990) "Sequence-specificity of the alkali-sensitive lesions induced in DNA by high intensity ultraviolet laser radiation", *Photochem. Photobiol.* **52**:509-517

Kroeber, D.W., and LaForge, R.L. (1980) *The Manager's Guide to Statistics and Quantitative Methods*, pp 81-92, McGraw-Hill Book Company, New York

Lamola, A. (1970) "Triplet Photosensitization and the Photobiology of Thymine Dimers in DNA", *Pure Appl. Chem.* **24**:599-610

Lamola, A.A., and Eisinger, J. (1971) "Excited States of Nucleotides in Water at Room Temperature", *Biochim. Biophys. Acta* **240**:313-325

Letokhov, V.S. (1983) "Laser-Induced Chemistry", *Nature* **305**:103-108

Maniatis, T., Fritsch, E.F., and Sambrook, J. (1982) *Molecular Cloning: A Laboratory Manual*, Cold Spring Harbor Laboratories, Cold Spring Harbor, New York

Marquardt, D.W. (1963) "An algorithm for least-squares estimation of non-linear parameters", *J. Soc. Indust. Appl. Math.* 11:431-441

Masnyk, T.W., Nguyen, H.T., and Minton, K.W. (1989) "Reduced formation of bipyrimidine photoproducts in DNA UV irradiated at high intensity", *J. Biol. Chem.* 264:2482-2488

Menshonkova, T., Simukova, N., Budowsky, E., and Rubin, L. (1980) "The effect on high-intensity ultraviolet irradiation on nucleic acids and their components: cleavage of N-glycosidic bond in thymidine, adenine, and 2'-deoxyadenosine", *FEBS Lett.* 112:299-301

Minton, K.W., and Friedberg, E.C. (1974) "Evidence for clustering of pyrimidine dimers on opposite strands of UV irradiated bacteriophage DNA", *Int. J. Radiat. Biol.* 26:81-85

Moore, W.J. (1962) *Physical Chemistry* (3 ed.) pp 457-616, Prentice Hall, Englewood Cliffs, NJ

Moroson, H., and Alexander, P. (1961) "Changes produced by ultraviolet light in the presence and in the absence of oxygen on the physical chemical properties of deoxyribonucleic acid", *Radiat. Res.* 14:29-49

Nguyen, H., and Minton, K. (1988) "Ultraviolet-induced Dimerization of Non-adjacent Pyrimidines- A Potential Mechanism for the Targeted -1 Frameshift Mutation" *J. Mol. Biol.* 200:681-693

Nikogosyan, D.N., Angelov, D.A., and Oraevsky, A.A. (1982) "Determination of parameters of excited states of DNA and RNA bases by laser UV photolysis", *Photochem. Photobiol.* 35:627-635

Nikogosyan, D.N., and Gurzadyan, G.G. (1984) "Two-quantum photoprocesses in DNA and RNA biopolymers under powerful picosecond laser UV irradiation", *Laser Chem.* 4:297-303

Nikogosyan, D.N. (1990) "Two-quantum UV photochemistry of nucleic acids: comparison with conventional low-intensity UV photochemistry and radiation chemistry," *Int. J. Radiat. Biol.* 57:233-299

Opitz, J., and Shulte-Frohlinde, D. (1987) "Laser-induced photoionization and single-strand break formation for polynucleotides and single-stranded DNA in aqueous solution: model studies for the direct effect of high energy radiation on DNA", *J. Photochemistry* 39:145-163

Oraevsky, A., Sharkov, A., and Nikogosyan, N. (1981) "Picosecond Study of Electronically Excited Singlet States of Nucleic Acid Components", *Chem. Phys. Lett.* 83:276-280

Patrick, M.H., and Rahn, R.O. (1976) "Photochemistry of DNA and Polynucleotides: Photoproducts", in *Photochemistry and Photobiology of the Nucleic Acids* (Wang, S., ed) Vol. 2, pp 35-95, Academic Press, New York

Patrick, M.H. (1977) "Studies on Thymine-Derived UV Photoproducts in DNA- I. Formation and Biological Role of Pyrimidine Adducts in DNA", *Photochem. Photobiol.* 25:357-372

Pesce, A.J., Rosen, C., and Pasby, T. (1971) *Flourescence Spectroscopy*, pp 1-63, Marcel Dekker, New York

Pummer, H., Egger, H., and Rhodes, CH.K. (1984) "High-Spectral-Brightness Excimer Systems", in *Excimer Lasers* (Rhodes, Ch.K., ed) pp 217-228, Springer-Verlag, Berlin

Rahn, R.O., and Patrick, M.H. (1976) "Photochemistry of DNA: secondary structure, photosensitization, base substitution, and exogenous molecules", in *Photochemistry and Photobiology of the Nucleic Acids* (Wang, S., ed) Vol. 2, pp 97-145, Academic Press, New York

Rigler, R., Claesens, F., and Kristensen, O. (1985) "Picosecond Flourescence Spectroscopy in the Analysis of Structure and Motion of Biopolymers", *Anal. Instrum.* 14:525-546

Rubin, L.B., Menshonkova, T.N., Simukova, N.A., and Budovsky, E.I. (1981) "The Effects of High-Intensity UV-Radiation on Nucleic Acids and Their Components- I. Thymine", *Photochem. Photobiol.*, 34:339-344

Salet, C., and Bensasson, R. (1975) "Studies on Thymine and Uracil Triplet Excited State in Acetonitrile and Water", *Photochem. Photobiol.* 22:231-235

van der Schans, G.P., Bleichrodt, J.F., and Blok, Joh. (1973) "Contribution of various types of damage to inactivation of a biologically-active double-stranded circular DNA by gamma-radiation", *Int. J. Radiat. Biol.* 23:133-150

Scholes, G. (1976) "The Radiation Chemistry of Pyrimidines, Purines, and Related Substances", in *Photochemistry and Photobiology of Nucleic Acids* (Wang, S., ed) Vol 1, pp 521-577, Academic Press, New York

Schrager, R.I. (1972) "Quadratic programming for non-linear regression", *Commun. Assoc. Computing Machinery* 13:625-634

Schumaker, V.N., Richards, E.G., and Schachman, H.K. (1956) "A study of the kinetics of the enzymatic digestion of deoxyribonucleic acid", *J. Amer. Chem. Soc.* 78:4230-4236

Schulte-Frohlinde, D., Opitz, J., Görner, H., and Bothe, E. (1985) "Model studies for the direct effect of high-energy irradiation on DNA. Mechanism of strand break formation induced by laser photoionization of poly-U in aqueous solution", *Int.J. Radiat. Biol.* 48:397-408

Smith, L.B. (1970) "The use of interactive graphics to solve numerical problems", *Commun. Assoc. Computing Machinery* 13:625-634

von Sonntag, C., Hagen, U., Schön-Bopp, A., and Schulte-Frohlinde, D. (1981) "Radiation-Induced Strand Breaks in DNA: Chemical and Enzymatic Analysis of End Groups and Mechanistic Aspects", in *Advances in Radiation Biology* (Lett, J.T., and Adler, H., editors) Vol 9, pp 109-142, Academic Press, New York

Sutherland, J.C., and Sutherland, B.M. (1970) "Ethidium Bromide-DNA Complex: Wavelength Dependence of Pyrimidine Dimer Inhibition and Sensitized Fluorescence as Probes of Excited States", *Biopolymers* 9:639-653

Varghese, A., and Wang, S. (1967) "Ultraviolet Irradiation of DNA *in vitro* and *in vivo* Produces a Third Thymine-Derived Product", *Science* 156:955-977

Wang, S. (1976a) "Pyrimidine Bimolecular Photoproducts", in *Photochemistry and Photobiology of Nucleic Acids* (Wang, S., ed) Vol 1, pp 295-356, Academic Press, New York

Wang, S., editor (1976b) *Photochemistry and Photobiology of Nucleic Acids*, Academic Press, New York

Weidner, R.T., and Sells, R.L. (1968) *Elementary Modern Physics* (2 ed.) pp 165-315, Allyn and Bacon, Boston

Whillans, D., and Johns, H. (1971) "Properties of the Triplet States of Thymine and Uracil in Aqueous Solution", *J. Am. Chem. Soc.* 93:1358-1362

Zavilgelsky, G., Gurzadyan, G., and Nikogosyan, D. (1984) "Pyrimidine dimers, single-strand breaks and crosslinks induced in DNA by powerful laser UV irradiation", *Photobiochem. Photobiophys.* 8:175-187